U. S. DEPARTMENT OF COMMERCE
Luther H. Hodges, Secretary
WEATHER BUREAU
F. W. Reichelderfer, Chief

NATIONAL SEVERE STORMS PROJECT

REPORT No. 13

500-KC./SEC. SFERICS STUDIES IN SEVERE STORMS

by

Douglas A. Kohl and John E. Miller

General Mills, Inc., Minneapolis, Minnesota

A report on research conducted under contract Cwb-10346 between the U. S. Weather Bureau and General Mills, Inc. and in accordance with Project Agreement ARDS-A-176 between the Federal Aviation Agency and the Weather Bureau. This version has been abridged by Jean T. Lee of National Severe Storms Project from the original contract report which appeared earlier as General Mills, Inc., Report No. 2346.

Washington, D. C.
April 1963

Please note change of address for NSSP

NEW ADDRESS

National Severe Storms Project
Room 710, Federal Office Building
Kansas City 6, Missouri

CONTENTS

500-KC./SEC. SFERICS STUDIES IN SEVERE STORMS

Douglas A. Kohl and John E. Miller
General Mills, Inc., Minneapolis, Minnesota

ABSTRACT

The count rate of "sferics" monitored at 500 kilocycles per second has been related to severe weather events occurring within the detection area during a 48-day period. Sferics activity was always in evidence prior to and during severe weather occurrences. Few severe weather events occurred after the sferics count rate began to decrease. Radar evidence of "hard" echoes from the vicinity of a severe weather event occurred prior to a rapid increase in sferics which immediately preceded the event.

I. INTRODUCTION

The electromagnetic radiation spectrum produced by lightning and other lightning-related discharges occurring during cumulonimbus cloud activity has been detected at monitor frequencies ranging from very low frequency (VLF) to microwave frequencies. An extensive attempt to relate VLF sferics[1] data to severe weather was made by the U. S. Air Force [1, 2]. The results indicated that although no apparent correlation existed at 10 kilocycles per second, some indication was in evidence at higher frequencies in the VLF spectrum. This finding supported the view held by Jones [3] that a severe weather event such as a tornado produces identifying changes in sferics count rate at monitor frequencies near 150 kc./sec. Malan [4] showed that many more "sferics" pulses are detected by monitoring at medium and high frequencies than at VLF. The use of medium frequency monitoring between 400 and 500 kc./sec. has proven to be a good compromise between long detection range and good response to thunderstorm characteristics [5]. In addition to sferics count rate as a parameter, changes in the amplitude distribution of 500-kc./sec. sferics have been related to thunderstorm development and a tornado evolution [6].

During the 1962 NSSP operational season, an omni-directional 500-kc./sec. sferics recorder was in operation at Shawnee, Okla., as well as the SPARSA (Sferic Pulse Amplitude Rate Spectrum Analyzer) equipment (fig. 1) developed by General Mills, Inc. This latter equipment also monitored sferics at 500-kc./sec.[2]

---

[1]The term "sferics" as used in this report refers to the electromagnetic radiation produced by all forms of electrical discharges occurring near or within lightning-related regions of charge separation in thunderstorms.

[2]Hereafter 500-kc. will be understood to mean 500-kc./sec.

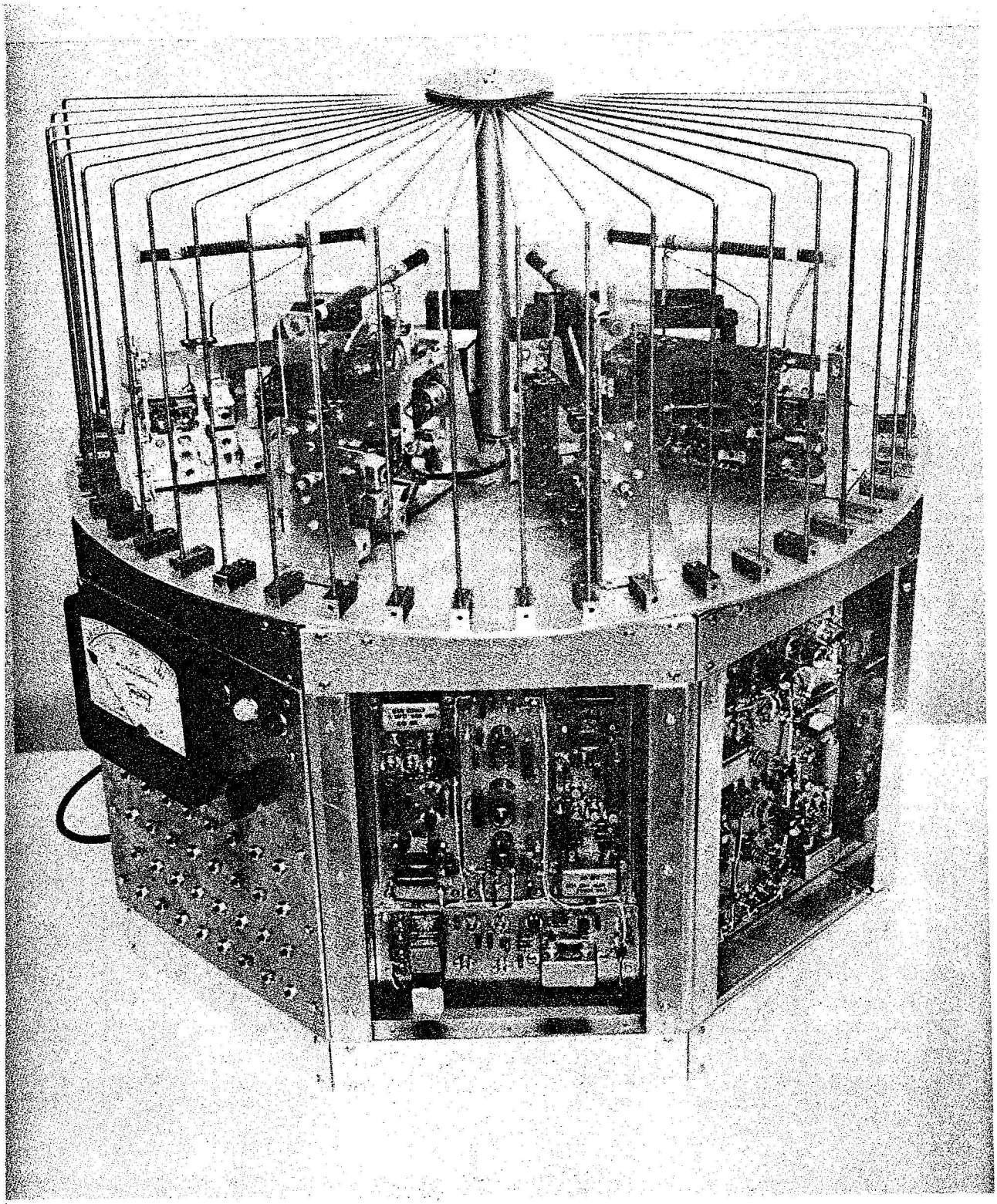

Figure 1.- Photograph of SPARSA equipment.

The antenna used in the SPARSA equipment is a ferrite core loop which has a core length of 7 inches. A nearly perfect cosine characteristic is obtained from such an antenna. Because of the large permeability of the core, only a very few turns of wire are required to obtain the proper tuned circuit inductance. Physically, therefore, the capacitive coupling from the winding to the electrical field is extremely low compared to larger air core loops. The low capacitive coupling rejects a large portion of the electrical vector component of incoming radiation, making the antenna voltage output proportional only to the magnetic component. Furthermore, the size of the antenna permits the use of small, low-loss Faraday shields that are very effective in rejecting local electrostatic sources of interference as well as near-field electrostatic sferic reflections from power lines, water pipes, and other metal objects.

The sensitivity pattern for the magnetic field of such an antenna is describable by the vector dot product between a vector perpendicular to the plane of the loop and the magnetic vector of the incident radiation. This cosine variation includes zero, which is normally used in direction finders to obtain azimuthal information. The SPARSA detector includes two antennas in order to achieve the special directional characteristics. This characteristic is based on geometrical field pattern orientation and corresponding, different output voltages. The circuit rejects all signals which do not arrive from within an arbitrary acceptance angle. Furthermore, it will not accept multi-path signals or those with certain polarizations. The elevation characteristic, however, is constant, and thus no discrimination of signals coming from different elevations will be possible because of the antenna's sensitivity pattern. An important feature of the instrument is that its directional properties are almost independent of sferic signal strength. The effective acceptance angle is for a 5.6° beam width. Only extremely intense signals which cause receiver limiting will effectively narrow the acceptance angle toward zero.

Signals arriving from directions outside of the acceptance angle are rejected, regardless of their amplitudes, even when they cause receiver limiting. Improper signals are never accepted; however, desirable signals may fail to be accepted due to coincidence loss. Simultaneous arrival of two or more signals results in the complete rejection of both. For example, if two storms within the detection range have two different absolute sferic counting rates, coincidence losses from their respective effects on each other's detection will bias the counting rates and increase the relative ratio between them.

The SPARSA equipment is designed to rotate automatically and provides an output of sferics count rate in each 5.6-degree sector subdivision of the azimuth circle. The detection system is characterized by a maximum detection range of about 200 n. mi. and a fair weather background count rate of zero. A pulse height distribution operator provides counting rates independent of range and has the effect of measuring only the nearest storm if several at different ranges are within the same sector.

The data analysis which is the subject of this report is concerned with the relationships which exist among the data obtained with sferics detection equipment of this kind, severe weather event reports, and weather radar echo analysis.

The severe-weather data used were furnished by the U. S. Weather Bureau (Kansas City) in the form of date, time, location, kind of severe weather occurrence, and source of the report.

A WSR-57 radar at Will Rogers Airport, Oklahoma City, Okla. (OKC) furnished the radar information during field operations and for film studies later. This radar, participating in the National Severe Storms Project (NSSP), is used as a common parameter in relating various other storm research programs, as well as a guide in operations.

The scope of the material covered is limited, not by the amount of data obtained, but by the amount of time allocated for processing and study. Because very few data have been reported in the technical literature concerning medium-frequency sferics monitoring, the data analysis has been performed to answer the following basic questions:

1. Can severe weather occur without 500-kc. sferics activity?
2. Is there any correlation between severe weather incidents and 500-kc. sferics activity?
3. Is 500-kc. sferics activity originating in the same area as the radar echo?
4. Is there any correlation between precipitation distribution and density, and 500-kc. sferics activity?
5. In what way is 500-kc. sferics activity related to thunderstorm dynamics, turbulence, etc.?
6. Are 500-kc. sferics data redundant with radar data?

It is recognized that the scope of this report is limited by restricting the study to severe weather location references and to radar and that the full meaning of some of the results cannot be understood until more data are utilized.

II. SUMMARY OF OPERATIONS

The operation of the Shawnee, Okla. SPARSA commenced at 1200 CST, May 12, and ended at 1330 CST, June 29. The second SPARSA, based in Arapaho, Okla., was installed on May 22. During this period General Mills' personnel were in attendance at each station to perform data analysis and assure functioning of the equipment.

A. LOCATION

The locations of the SPARSA units were primarily chosen to permit triangulation over the NSSP Alpha and Beta surface networks with large angles of intersection. Shawnee, 39 miles from the OKC radar, at one corner of the network, and Arapaho, 80 miles in the opposite direction, provided the proper geometry (fig. 2). All parts of the surface networks were within range of both units. Arapaho, OKC, and Shawnee are in a straight line extending nearly west to east.

It is considered more desirable to aline the SPARSA stations on a north-south line so they can better observe incoming weather systems; however, at the time, CW transmission from powerful, medium-frequency military transmitters to the south precluded the use of Gainesville, Tex., which had been investigated as the second site.

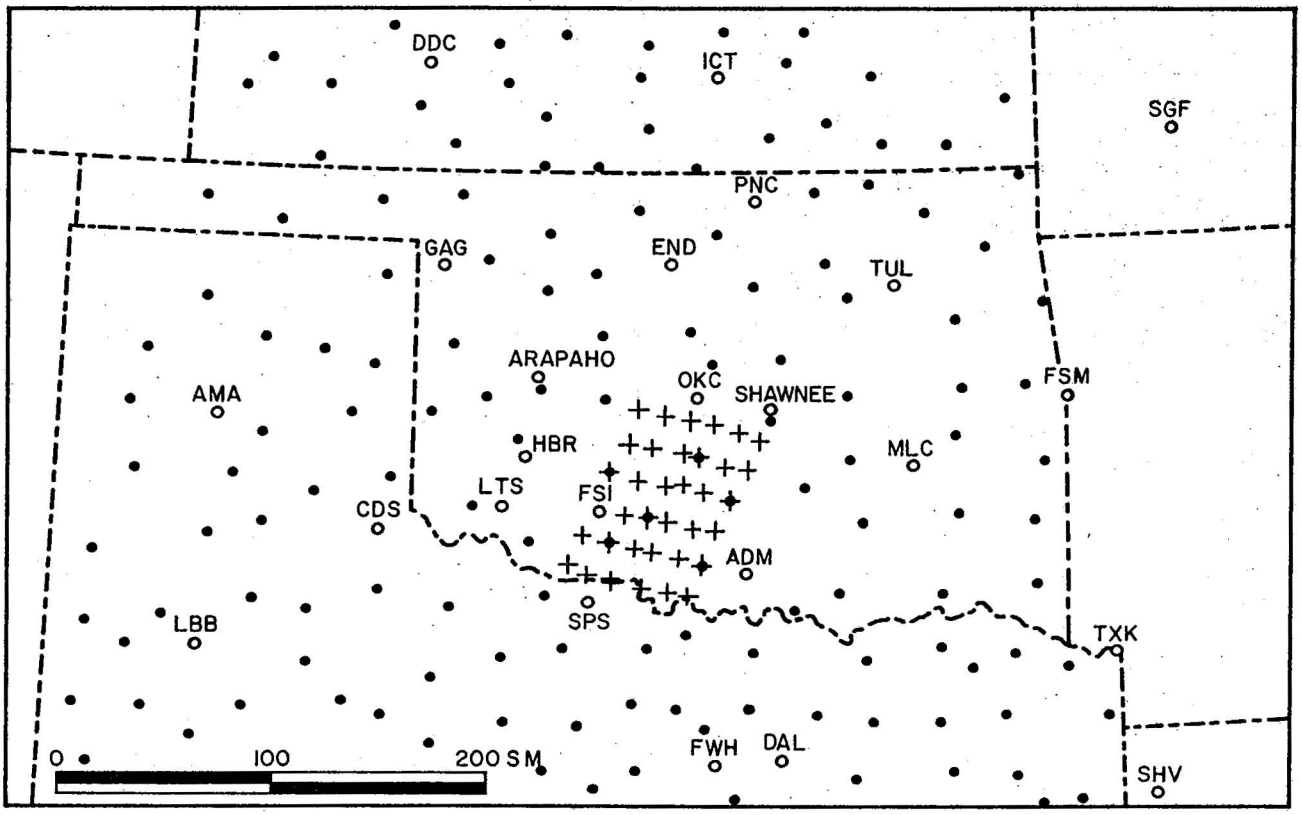

Figure 2.– Map showing relationship of SPARSA stations (Shawnee and Arapaho) to the α network stations (°) and β network stations (+).

B. HOURS OF OPERATION

At Shawnee, out of a total of 1152 hours of operation, there were 47 periods of 500-kc. sferics activity, totaling 821 hours. This means that 72 percent of the time, within the 200-mile radius of detection range, sferics activity was being produced. The result was the recording of 9120 blocks (0° to 360°) of sferics data.

C. EQUIPMENT PERFORMANCE

The combined operation total of both SPARSA units was 2112 hours of ON time. A summary of equipment problems is as follows:

Operating Failures	Functional Problems
20 electrical	9 wiring errors
2 mechanical	3 major adjustments

The equipments were new and had not been field tested before installation in Oklahoma; hence the undetected wiring errors which were to be corrected later. Major adjustments were necessary to eliminate the radio-frequency code interference in the region.

III. DATA ANALYSIS

The answers to the basic questions formulated in the Introduction required a rather diverse approach to data analysis. The study of severe-weather relationships was accomplished, using data from each day's operation. However, other studies have necessarily been restricted to a few storms with a more thorough and complete evaluation of each.

A. 500-KC. SFERICS (OMNI-DIRECTIONAL) AND SEVERE-WEATHER RELATIONSHIPS

The presence of sferics activity and its level were examined with respect to the official tabulation of severe-weather events.

1. *Summary Data*

Omni-directional relationships. The detection area is quite similar in extent to that of the radar and includes about 130,000 square miles. Thunderstorms occurring anywhere in the region contribute their respective sferics activity to the total or omni-directional count rate as measured at the monitor point. The severe weather incidents which occurred within the same detection area were used for the comparison with the sferics activity.

At the far left side of figure 3 is the record of duration of omni-directional total sferics activity distributed according to the calendar. The basis is from midnight to midnight at Shawnee, Okla.

Sferics activity was evident every day. This is not unusual for this latitude during the months of May and June as it represents the response from a storm anywhere within the detection area -- roughly extending to Dallas, Tex., on the south; Hot Springs, Ark., on the east; beyond Hutchinson, Kans., on the north; and nearly to Amarillo, Tex., on the west. The total number of sferics pulses detected per day shows a much greater variation and reflects considerable differences in count rate (fig. 3).

2. *Quantitative Relationships*

The histograms in the center of figure 3 portray the distribution of severe-weather reports and total sferics counts per day among the various calendar days. Out of all of the severe-weather reports compiled, only those occurring within a radius of 200 n. mi. of Shawnee are tabulated.

Since a larger area is included by an incremental increase in radius at 200 miles, as compared to 20 miles, the rather even and broad distribution in distance from the detection station to the severe weather event (fig. 4) may be due, in part, to some psychological bias in the reporting of the weather incidents in the central area. In figure 3 the total 500-kc. sferic counts per day are shown quantized to 250,000 pulse units. An average count rate may be obtained by dividing the total counts per day by the number of sferic hours per day. However, a more interesting concept is that of the rate-of-change of total sferics activity. These data are shown in the right-hand column.

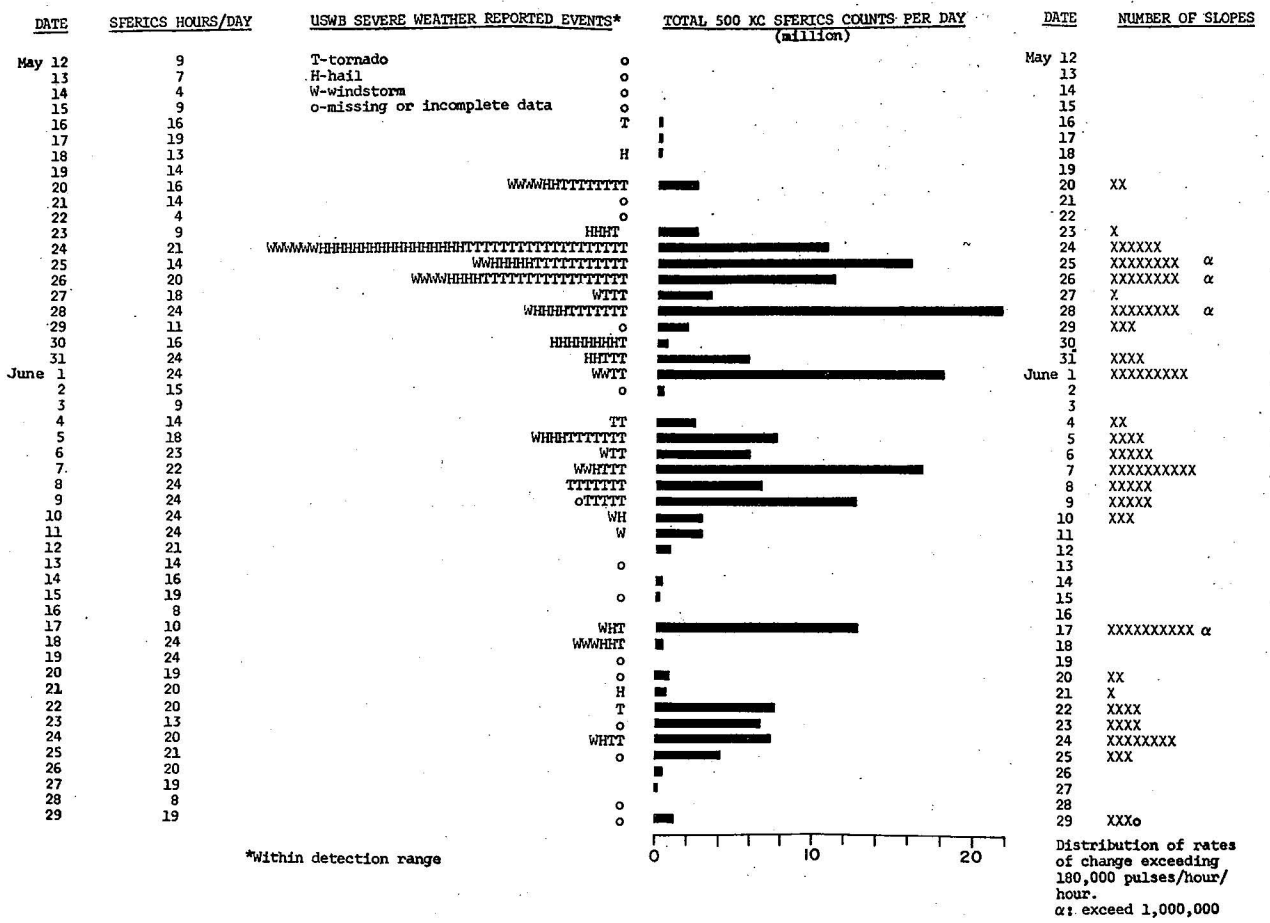

Figure 3.- Summary of omni-directional 500-kc. sferics and severe weather occurrences.

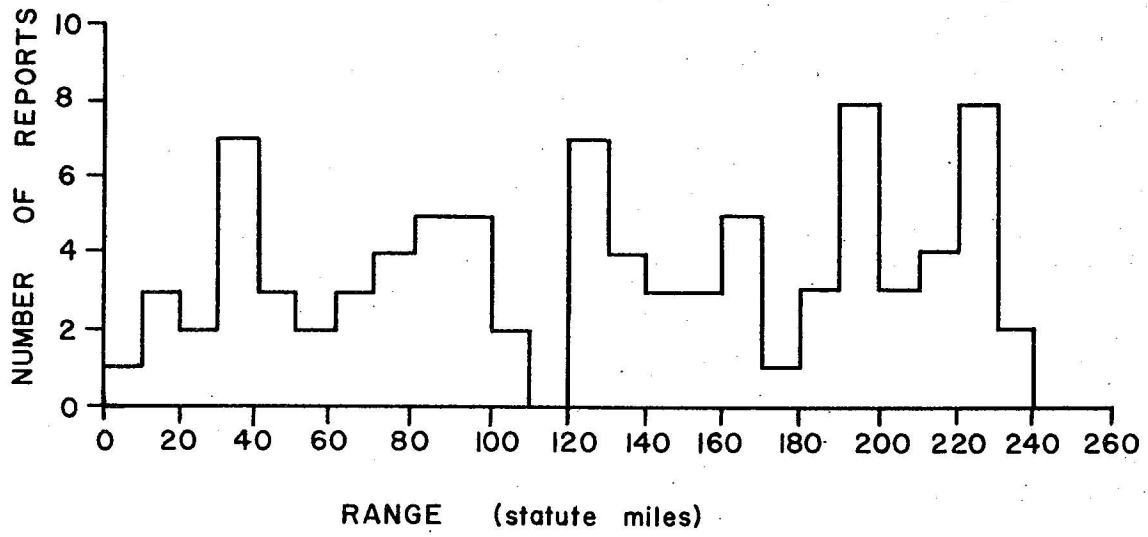

Figure 4.- Distribution of distance to severe weather occurrence from the sferics stations.

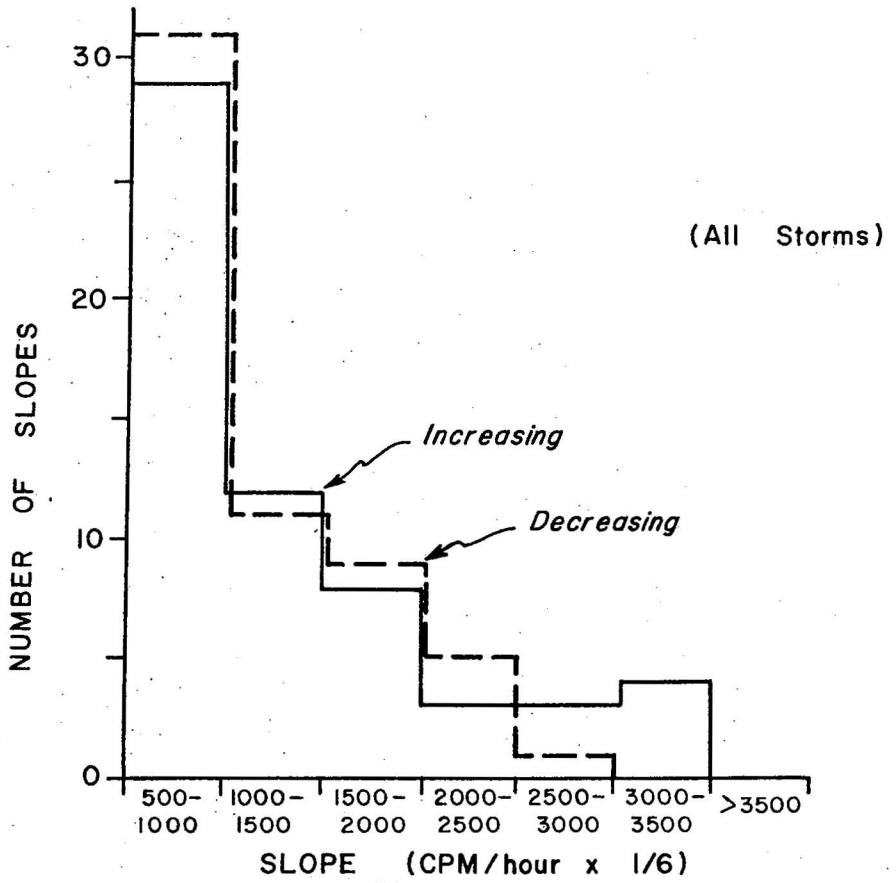

Figure 5.– Distribution of total 500-kc. sferics activity rate of change.

A further amplification of the data was performed to see whether on a regional basis, the transient aspect of the thunderstorm phenomenon has any time bias. The data in figure 5 are a distribution of the rates of change of sferics level obtained from the total omni-directional 500-kc. sferics count rate record. It is important in that it indicates that an onset of sferics activity is, on the average, no more rapid than the cessation of activity.

The slope of the general trend of sferics activity is important in defining the maximum level instant during a stormy period. A typical record of a sferics activity period is shown in figure 6. Note the rapid initial build-up of count rate from zero to over 15,000 counts per minute in less than 3 hours' time. The maximum activity (38,400 c.p.m.) is well defined in the record, and the time of occurrence is indicated by the dashed line. The times of occurrence of severe weather are also indicated. Note that most of the severe weather occurred prior to the sferics activity maximum. This phenomenon was apparent in other storm periods also, as shown in table 1 which includes 67 severe weather events taken from the period of high incidence from May 23 to May 27.

During the increasing and decreasing trends in total sferics activity, there are frequent changes in slope, including short-period reversals in sign, all of which describe a succession of minor maxima superimposed upon

the average slope or trend. These minor fluctuations may be due to large area portions of different thunderstorm complexes undergoing simultaneous changes in activity and will be discussed in the section concerned with directional sferics activity.

Table 1.- Severe Weather Incidence Related to Total Sferics Activity

Date and Time of Investigation	SW Events Occurring Prior to S_T Maximum	SW Events Occurring After S_T Maximum	Total Number of SW Events
1500 CST May 23, 1962 to 0600 CST May 24, 1962	4	0	4
1600 CST May 24, 1962 to 0440 CST May 25, 1962	25	5	30
1620 CST May 25, 1962 to 0800 CST May 26, 1962	14	5	19
1500 CST May 26, 1962 to 0810 CST May 27, 1962	13	1	14
Total	56	11	67
	84%	16%	100%

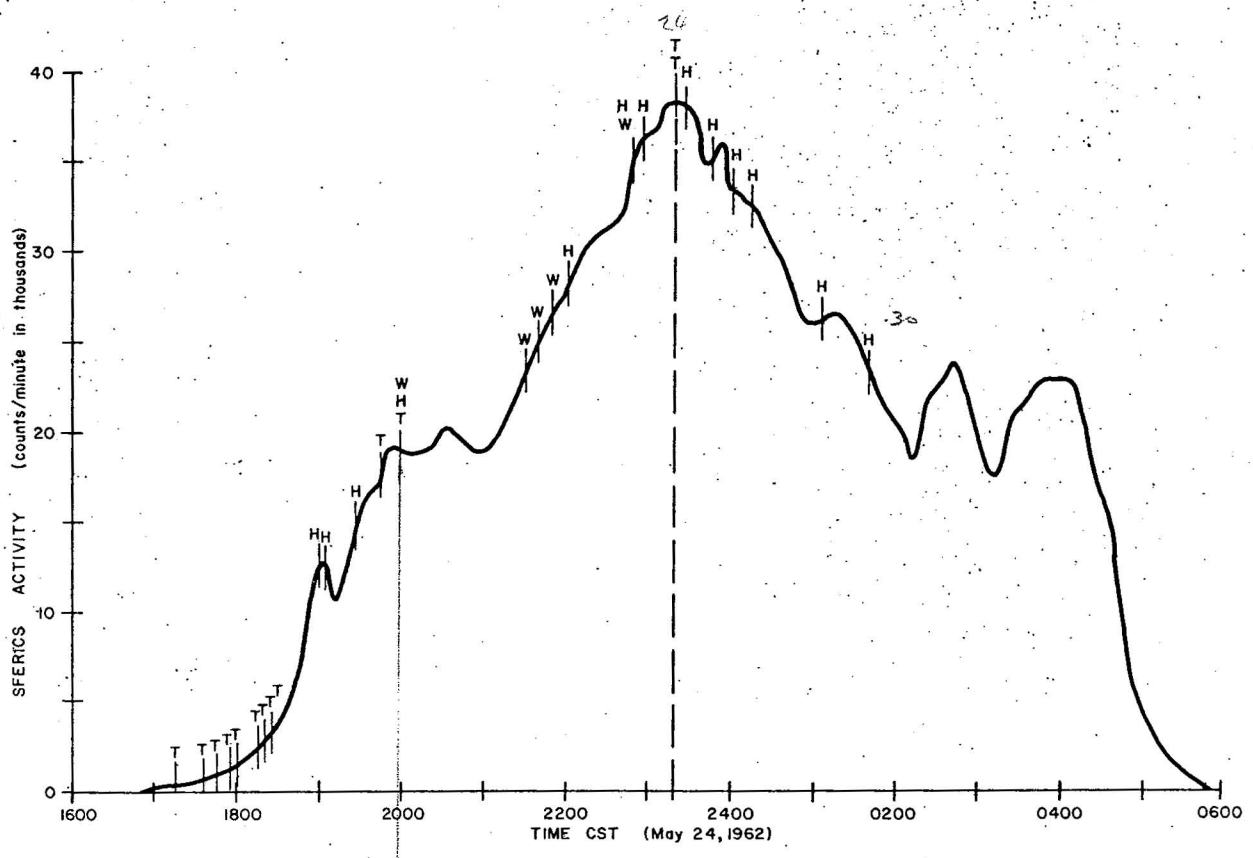

Figure 6.- Record of total sferics activity and severe weather occurrences for a typical day.

The distribution of time intervals between successive maxima in the total sferics activity from all storms which occurred during the 48-day period is shown in figure 7. On the basis of the distribution, it appears possible to predict when an overall storm period maximum has been attained. Observing 45 minutes of the record would give 50 percent probability; 60 minutes would give 75 percent probability; and 2 hours would approach 98 percent probability of determining the correct trend.

An indicator of the end of the occurrence of severe weather, therefore, may approach an accuracy of 84 percent if the period maximum may be defined and the accuracy in defining that maximum is dependent upon the observing interval. The time scale is considerably shortened when individual storm areas are observed as discussed in the next section. However, insufficient data have been analyzed to derive estimates of performance of various sferics measurements used in predictor fashion.

B. SPARSA AND SEVERE-WEATHER RELATIONSHIP

The previous results present the regional perspective on the relationship between severe weather and 500-kc. sferics. It is also important to perform azimuth sector comparisons because of the localized nature of severe storms. The directional sferics activity distribution was measured by monitoring equipment -- SPARSA -- which averaged the sferics count rate occurring in each of 32 azimuth sectors. The azimuth circle was quantized into 64 sectors, 5.6° wide; however, a 180° ambiguity exists in the equipment. The time and location of severe weather events were obtained from the severe weather logs. Individual severe weather events were referred to the directional sferics recording at the time of occurrence by identifying the azimuth sector containing the direction line to the event location. An analysis was performed on those severe weather events occurring between May 16 and May 27. Table 2 summarizes the results. The fact that the two instances of severe weather, which were apparently undetected, were tornadoes probably has no more significance than their long ranges.

Table 2.- Correlation Between Severe Weather Locations and 500-Kc. Sferics: Sector Basis

Total Number of SW Locations Checked (May 16 through 26)	Number of SW Locations Which Had 500-Kc. Sferics	Number of SW Locations Which Did NOT Have SA Due to Inoperative Equipment	Number of SW Locations Which Did NOT Have 500-Kc. Sferics Activity
87	80	5	2*
100%	92%	5.7%	2.3%

*May 24, 1637 CST. Tornado NW Hutchinson, Kans., 205 miles. (Note: Sectors on both sides of the one containing this location did contain sferics activity.)

*May 26, 1915 CST. Tornado N Emporia, Kans., 220 miles.

Most of the severe weather events did not occur simultaneously in pairs or combinations, so the significance of the sferics level in the sector containing the location was tested by relating it to the maximum sferics level

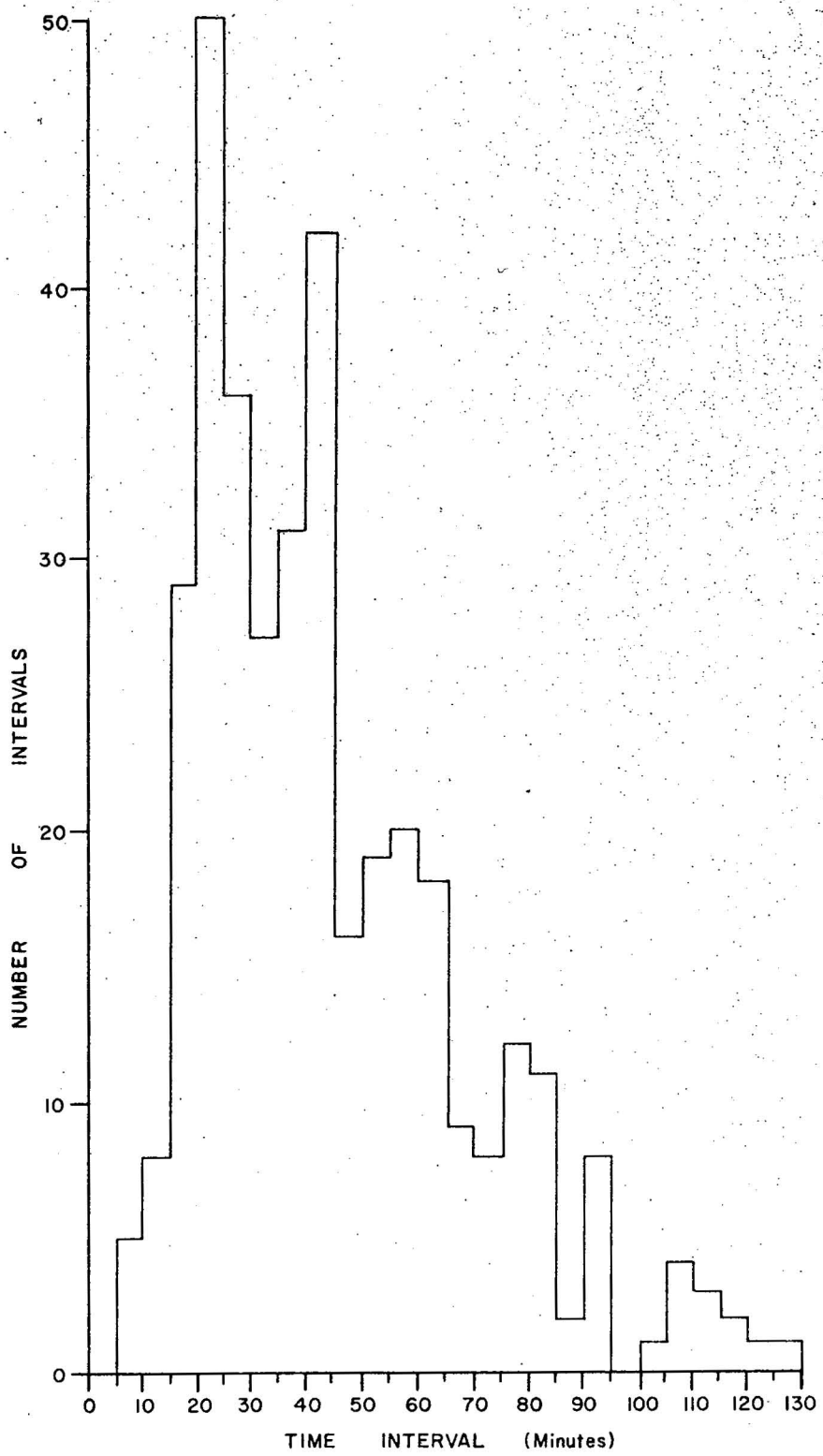

Figure 7.- Time interval between maxima of 500-kc. sferics count rate.

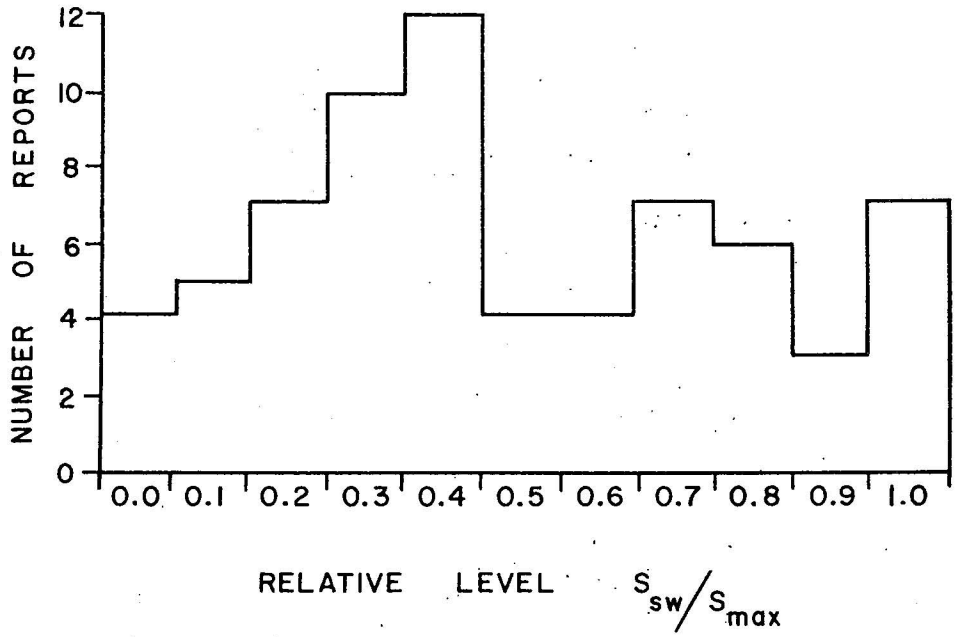

Figure 8.- Distribution of relative sferics levels at time of severe weather events where relative sferics level is sferics count at time of severe weather event (S_{SW}) divided by maximum sferics count (S_{max}).

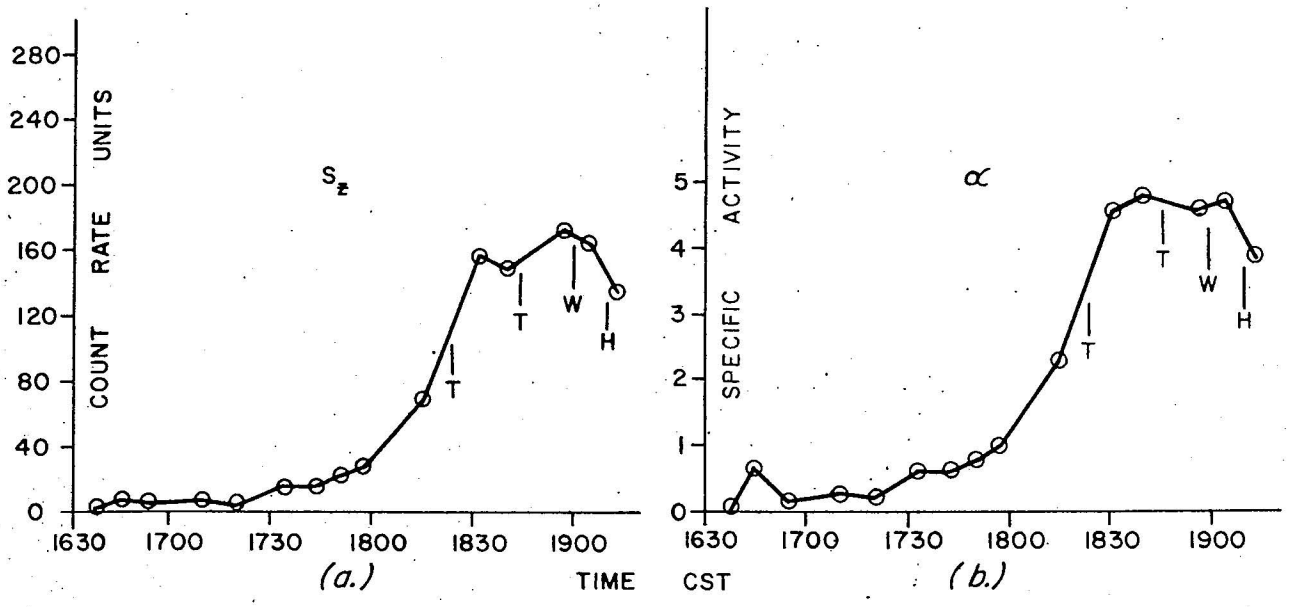

Figure 9.- (a) Sferics activity in sector with severe weather (SW) where T indicates tornado, W a windstorm, and H indicates hail at time of occurrence, May 25, 1962. (b) Specific activity (α) in sector with severe weather, May 25, 1962.

observed at that time at any azimuth. These data are found in figure 8 in the form of a distribution of the fractional activity level: the sferics count rate in the SW sector divided by the sferics count rate maximum of any sector. Although the sferics activity may be appreciable in the vicinity of the severe weather location, it is not large enough to permit reliable identification in the great variety of storm configurations and evolutions that occur. This is in part due to the fact that different storms are in various stages of maturity and dissipation and thus, as will be discussed later, the individual history of activity within each sector is an important parameter.

Figure 9 shows a typical history of the sferics activity in a sector in which severe weather occurs. The time and kind of each event is indicated on the graph. It is important to note that documented evidence of severe weather does not exist prior to the period of rapid sferics activity increase. This effect is also apparent for overall activity from all storms in the region as detected on the omni-directional basis previously mentioned.

C. SPARSA AND WEATHER-RADAR RELATIONSHIPS

The relationships derived between 500-kc. sferics and the WSR-57 radar echo distributions are based upon the common coordinate conversion of the echo location into the corresponding SPARSA azimuth sector within the detection range of SPARSA. Radar measures microwave reflectance of scattering and absorbing media within the total volume of the antenna pattern which is a parameter physically different from that of the SPARSA output. The sferics count rate for any SPARSA sector arises from all electrical-type sources located within the sector regardless of altitude so that the detection volume is approximately wedge shaped.

The SPARSA output level is fundamentally derived from the number of sferic occurrences per unit of time. The actual solid angle or total volume of the storm does contribute to the output by increasing the absolute number of electrical-discharge locations possible. The acceptance angle of SPARSA, 5.6°, is preserved by scanning in steps. The WSR-57 effective beam width for large sources is increased to nearly the same value so that if the two equipments were at the same locations, the volumes surveyed for distant storms would be somewhat similar.

As indicated earlier, SPARSA does not count all the 500-kc. sferics produced within the acceptance angle, but the fraction counted tends to be independent of distance. The count rate does depend upon the pulse amplitude distribution, and although this is variable from storm to storm and with stages of maturity, no compensation for these absolute differences has been applied to the SPARSA data. One further characteristic is important. The visible lightning or return stroke and its associated pre-discharge and relaxation phases result in a large number of 500-kc. sferics closely spaced in time. The SPARSA-counting circuit recognizes this event and counts each return stroke as a single pulse.

1. *500-Kc. Sferics Origin as Defined by Radar*

Cumulonimbus cloud formations quite often appear as isolated events on the radar screen. It is possible, therefore, to define the sferics signal origins in terms of these echoes by assigning a single cloud portion to an

azimuth sector in SPARSA coordinates. The determination of the cloud echo or echoes to be assigned to a SPARSA sector is simply delineated by the sector limits and their intersection with the echo, as shown in figure 10.

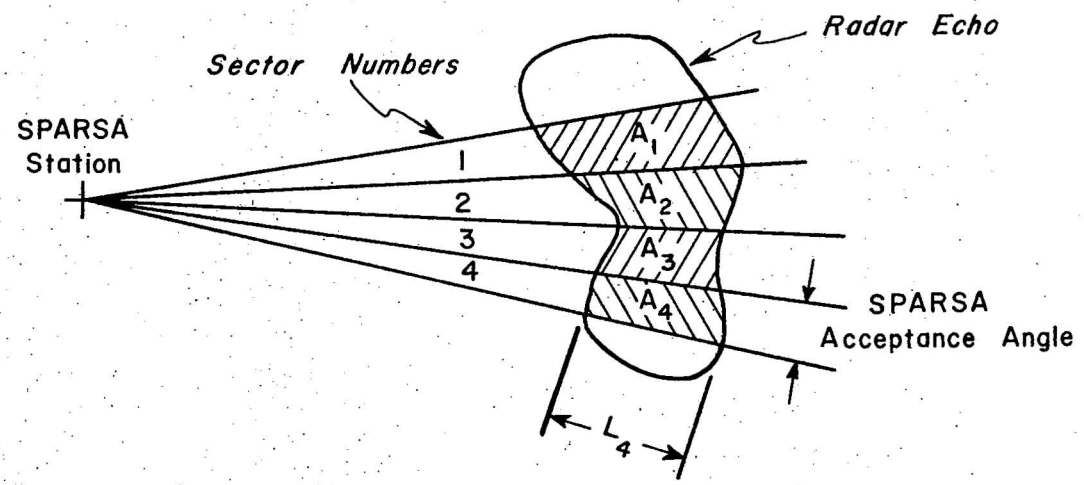

Figure 10.– Sferics-radar correlation parameters.

For each SPARSA sector values can be assigned corresponding to (1) sferics level, S; (2) cloud area, A; (3) cloud length, L; and (4) absolute radar reflectance, Z. Quantitative relationships have been derived on this basis; however, it is first necessary to establish the incidence of sferics with radar origin confirmation in order to justify quantitative results.

a. *Sector Analysis*

During the periods when 500-kc. sferics were present, the total number of SPARSA sectors which intersected radar echoes (taken at maximum gain) was tabulated. These data are shown in table 3.

Table 3.– 500-Kc. Sferics Origin Comparison With Total Weather Radar Echoes

Date	Number of Sectors With Both Sferics and Radar Echoes	Number of Sectors With Sferics but Not Radar Echoes	Number of Sectors With Radar Echoes but Not Sferics	Total Number of Sectors With Radar Echoes*
May 23	87	19	34	121
24	224	25	37	261
26	160	16	123	283
June 10	168	12	153	321
11	300	15	823	1123
12	249	33	482	731
Total	1188	120	1652	2741
	42%	4%	58%	100%

*WSR-57 Maximum Sensitivity; uncompensated for range; low antenna angle.

In the comparisons of table 3, it is valid not to compute absolute reflectance because the sectors containing echoes only or sferics only were adjacent to sectors containing both sferics and echoes and all intersecting a common storm area.

The variation of the proportion of sferics, their origin sectors, and total radar echo area are shown for two representative periods in figure 11. The data for June 12 show a proportionality between the total sferics level and the number of sectors with both sferics and radar echoes during the incipient stage and during the diminishing phase. This is also apparent in the data for June 10 which include just the middle and diminishing phases of the storm. Note that there are periods during which neither the total radar echo area nor the portion of the radar echoes producing sferics increases although there are very large increases in sferics level.

This leads to a method of expressing sferics activity in terms of specific activity based on area; specific activity, α, is thus the counts per minute per square mile of radar echo common to the sferics sector. In figure 9b the specific activity, α, is plotted for the same period as for 9a, for storms occurring on May 25, 1962. The specific activity also shows a rapid increase during the period of severe weather occurrence. The rapid rise in α is an indication that the sferics count rate is increasing much more rapidly than the radar echo area. (See also fig. 18.)

In the tabulation of table 3, 91 percent of the sectors with sferics activity also contained radar echoes. This portion of the data is of interest when analyzed as shown in table 4.

Table 4.- 500-Kc. Sferics Origin as Indicated by Weather Radar Echo in Sferics Sectors

Date	Number of Sectors With Both Sferics and Radar Echoes at Time: t	Number of Sectors With Both Sferics and Radar Echoes at Time: t ± 1hr.	Number of Sectors With Sferics Activity ONLY	Number of Sectors With Sferics Activity
May 23	87	7	12	106
24	224	24	1	249
26	160	14	2	176
June 10	168	12	0	180
11	300	15	0	315
12	249	23	10	282
Total	1188	95	25	1308
	90.8%	7.3%	1.9%	100%

The occurrence of sferics without radar echo in a sector in most cases arises from an area which previously did have both sferics and cloud echoes or in a building area in which echoes will later form and persist. Applying a time bracket of ± 1 hour to the sector comparison is an approximation to three times the standard deviation of the actual time differences which

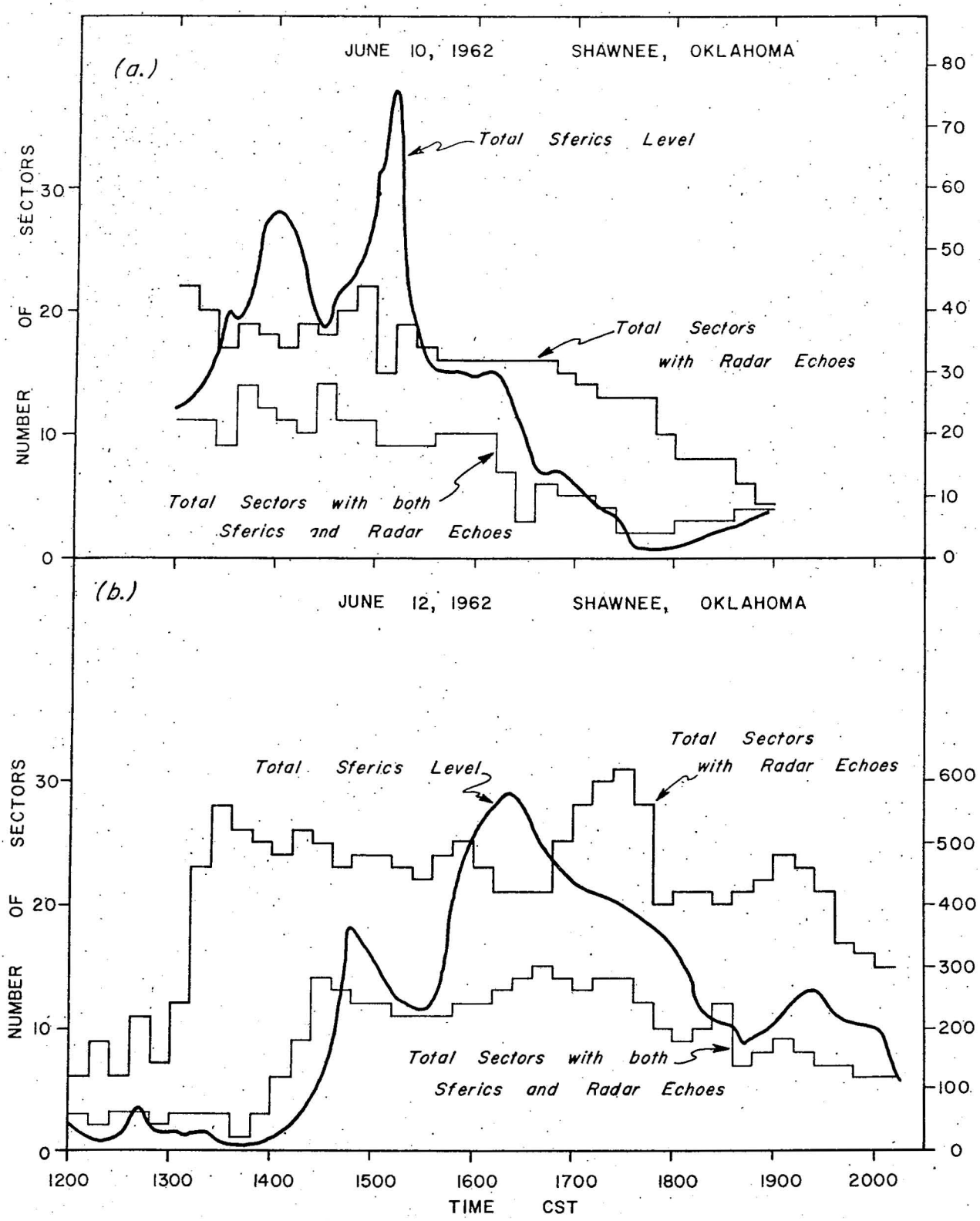

Figure 11.– Dynamic record of 500-kc. sferics and radar origins, June 10 and 12, 1962.

existed between the occurrence of sferics and the first (or last) evidence of echo in the sector.

In summary, 98.1 percent of the sectors measured which had sferics activity also contained radar cloud echoes. However, less than half of the radar echoes, even during advanced thunderstorm stages, were producing sferics. These facts, combined with those shown in table 2, appear to indicate that there is a close relationship between severe weather occurrences and radar echoes coincident with 500-kc. sferics. Further data are needed to substantiate the suggestion that if the radar echo is not coincident with 500-kc. sferics, the probability of severe weather occurring with this echo is small.

b. *Storm History*

On June 11, 1962, an isolated afternoon thunderstorm system formed close enough (50 to 100 mi.) to the Shawnee location to enable theodolite, photographic, and sferics measurements to be performed simultaneously. A large number of photographs, sferics "scans", and radar scans were made. Samples of the sferics data and radar plot are shown by figures 12 and 13.

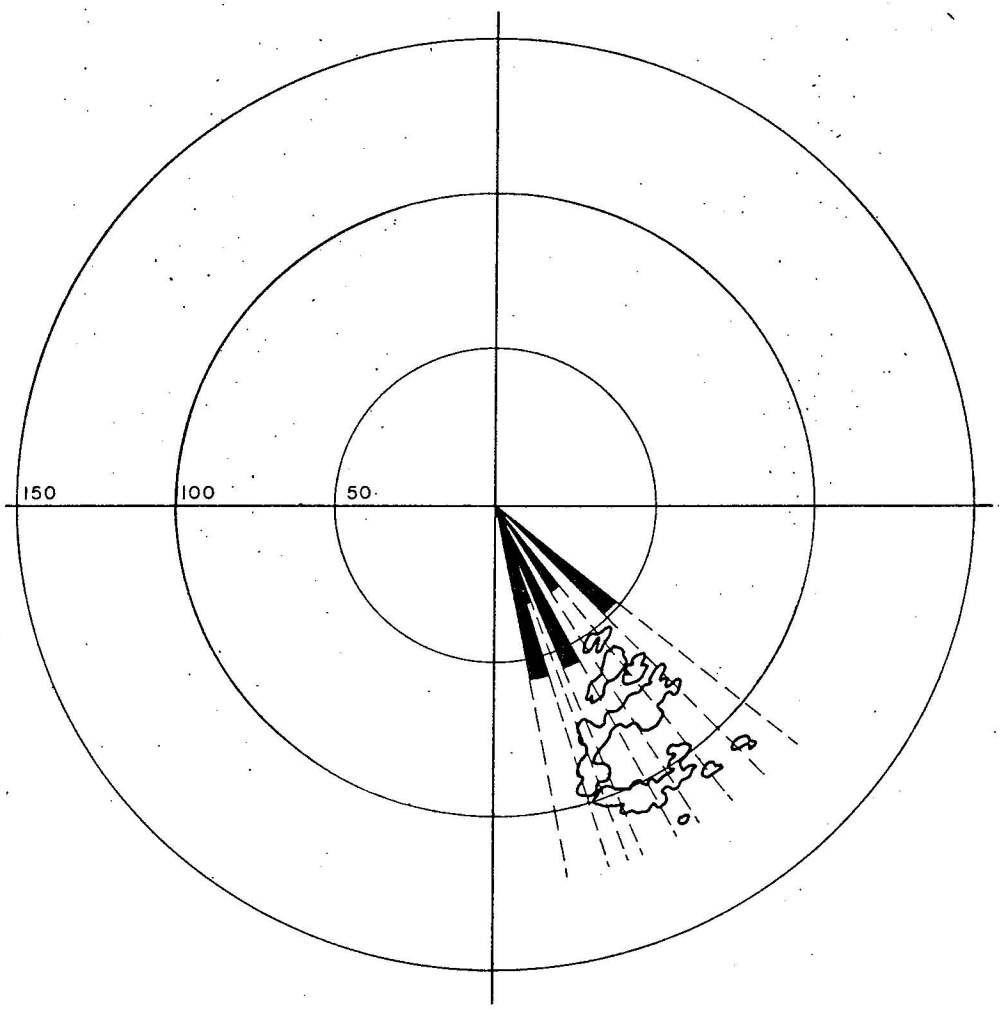

Figure 12.- Sample polar plot of sferics and radar echoes for June 11, 1962, at 1517 CST. Length of sferics bar indicates relative number of sferics in sector.

The sferics level is shown on a series of polar plots which also delineate the weather radar echo contours at the time. The length of the radius is proportional to the sector count rate.

The storm was an "air mass" storm which had formed at 1150 CST in a comparatively clear environment. The total duration of the electrical activity of the storm was 2 hours and 35 minutes, commencing at 1335 CST. Thunderstorms and heavy rain were reported at Hugo, Okla. (140°, 105 n. mi.), and Paris, Tex. (145°, 122 n. mi. from Shawnee) as part of the storm developing at the farthest range.

Several aspects of this series are of interest. High sferics activity consistently appeared in the sector which contained the western edge or "sunny side" buildup of vertically rising convective cells evidenced by the perpendicular cloud walls.

Maximum sferics level from the entire storm occurred at 1545 CST. This was followed by a sharp decline to zero in about an hour. During this decreasing activity period, however, a short-lived increase in activity occurred

Figure 13.- Sample polar plot of sferics and radar echoes for June 11, 1962, at 1555 CST. Length of sferics bar indicates relative number of sferics in sector.

in the sector where heavy thunderstorm activity was present, at Hugo and Paris. A number of storms were similarly investigated and the data combined as in figures 9, 18, and 19.

c. *Dynamics*

In the sector analysis to confirm sferics origin (refer to table 4), it was established that sferics activity may precede or persist after cloud echo changes. A further analysis of some aspects of dynamical relationships relative to sferics origin is warranted.

(1) *Cloud buildup prediction.* Nearly 3/4 of the sectors which proved to have sferics but not radar evidence of clouds were demonstrated to contain cloud echoes within a short time period. (Refer to tables 3 and 4.) The time interval, Δt, is the length of time which existed between the earliest evidence of cloud presence by radar and the advent of sferics activity. This distribution is given in figure 14.

Nearly all of the positive Δt values are associated with an increasing total area in those sectors with sferics activity as indicated by the I symbol. Conversely, nearly all of the negative values were associated with decreasing sferics-area, D. The presence of sferics without cloud echo, therefore, may indicate a region of cloud growth if the sector areas which already have sferics activity also show increasing area, or it may indicate the edge of a region of cloud dissipation if the sector areas which already have sferics activity also show decreasing area.

No estimate was made of the possible relationship between rate of cloud growth, sferics level, and prediction interval.

Nearly 2 percent of the sectors with sferics activity never contained any radar echoes. The percentage in this category varies with different storms and different locations. In some instances the number of sectors without radar confirmation of origin approaches 11 percent and in others, zero.

Visual evidence of the relationship between the onset of sferics activity and vertical convection with subsequent enlargement of radar echo return has already been mentioned. Other visual observations also support the finding that the type of cloud growth predicted by sferics activity is in the form of a rapidly ascending turret indicating strong vertical convection transport.

(2) *Rate of change of activity.* Maximum rates of change of sferics level tend to parallel maximum rates of change of cloud echo only during the initial phases of storm activity. It is during this early period of sferics activity increase, however, that the probability of severe weather is the greatest and also the fractional increase in total radar echo is greatest (see Sec. III, C). As indicated in the slope distribution of figure 5, total sferics activity increases and decreases occur at the same rate, on the average. This is not true of total radar cloud cover formed from the cumulonimbus process. In fact, in this study a number of severe weather occurrences were located near, but not within, a cloud echo area, but later stages of precipitation spread out to cover large areas with gradual depletion.

I = total sferics-cloud area increasing
D = total sferics-cloud area decreasing

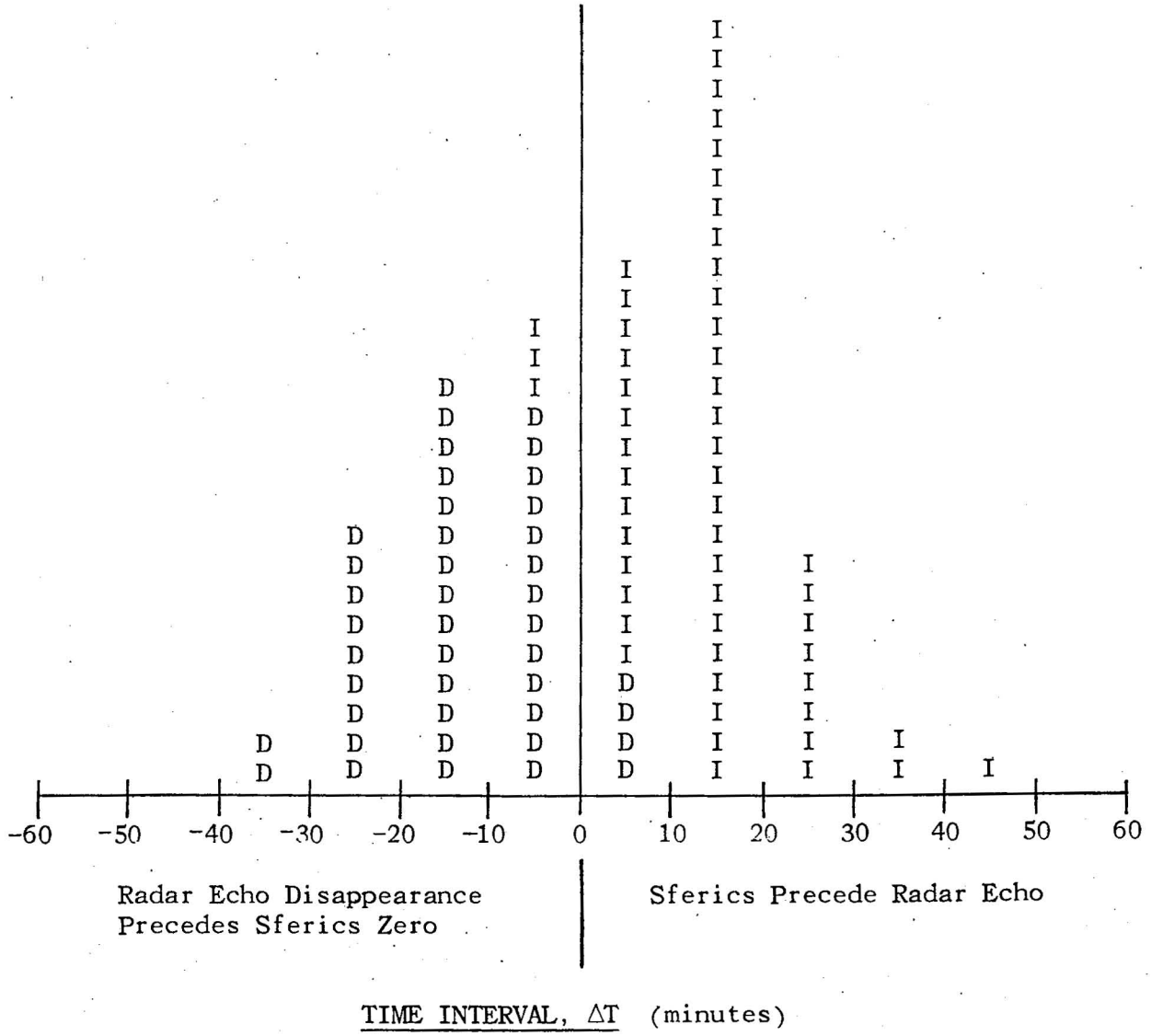

Figure 14.- Distribution of the time interval (Δt) between the occurrence of sferics activity and appearance of radar echo.

A further demonstration of the fact that sferics increases tend to parallel echo area increases only during the growing stages of a storm will be found in the effect of maturity upon the sferics-area correlation coefficients discussed in a later section.

Another interesting feature noticed was that although the relative levels of different portions of the cloud continually changed, there were instances in which all sectors showed simultaneous trends in count rate change.

The data shown in figure 15 were obtained from an extended single storm complex which lengthened out to cover 200 miles in an arc so that the axis of the storm was on a radius of about 100 miles from the Shawnee location. The SPARSA sectors represented sections through the storm about 10 miles wide. The times at which each sector showed a maximum sferics count are indicated. The times at which the total activity showed a maximum are indicated in the column at the right side of the figure. The significant finding is that a number of sectors simultaneously undergo maximum fluctuations. At 1445 CST, for example, nearly 60 miles of storm showed a simultaneous change in activity extending over 680 square miles. This is a very large area compared to the radar-defined individual cell. Time has not permitted an analysis of many of these occasions.

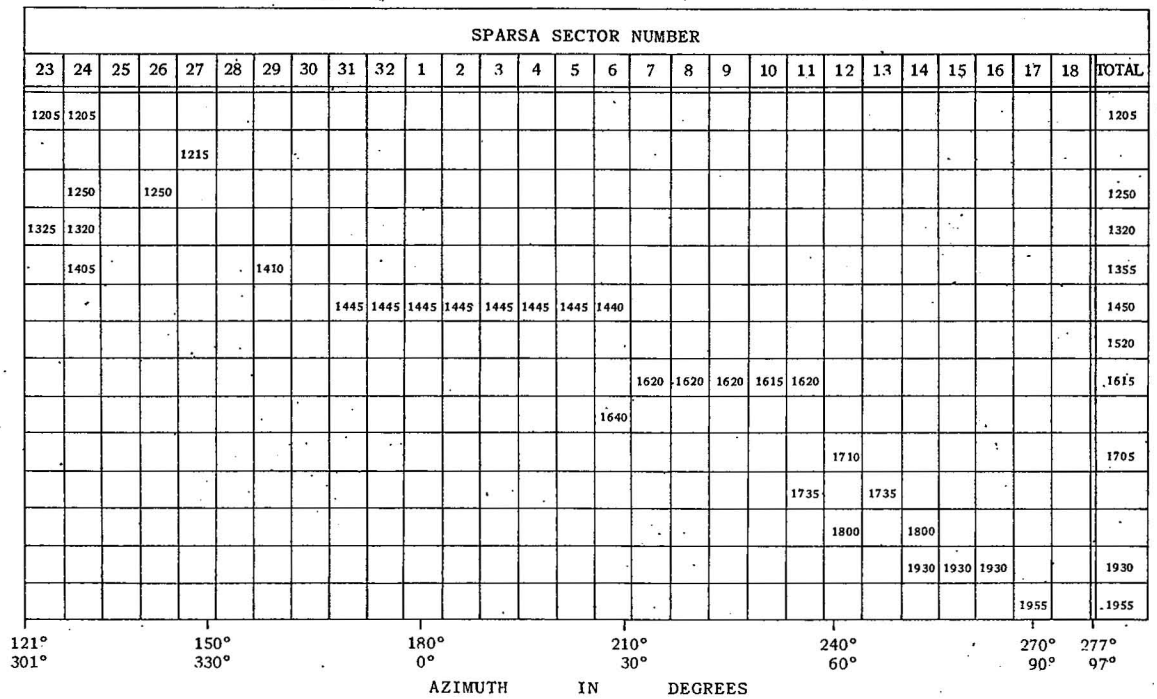

Figure 15.- Identification of sources (sectors) of sferics level maximum for a typical day. The time (CST) is given corresponding to 500-kc. sferics level maxima instants during the SPARSA record for each azimuth increment. The times of total activity (omni-directional) maxima appear in the right-hand column.

d. *Qualitative Relationships*

In terms of the actual presence of storms and their cloud formation manifestations, both radar and sferics detection are capable of a limited amount of qualitative analysis. The SPARSA units employed in these field tests were not used in a manner which would exploit their potential qualitative discrimination.

(1) *Relative information content.* Areas of different activity have been related to different levels of reflectance with radar analysis. This becomes a screening process. It can be shown that, by the step-gain procedure (as given in the original report), about 55 percent of the echo area is disregarded with step 1 gain reduction, 73 percent for step 2, and so on, until by step 5, 95 percent of the original echo area is lost.

The identification of cloud areas by sferics also reduces the area of interest by an average of 58 percent in terms of radar echo (see table 3). This is the equivalent of a 13.2 db. gain reduction of the radar receiver or about step 1 sensitivity.

This comparison cannot be generalized unless absolute reflectance values are used, but it is probably representative because the data of table 3 were obtained over a wide variety of distances, storm intensities, and stages of storm maturity.

(2) *Sector analysis.* The radar discrimination of localized intense precipitation and/or high absolute reflectance is increased by gain reduction. Sferics level is a time dependent term in the form of count rate. A comparison of areas of high precipitation rate with areas of high sferics activity is of interest. Without qualifying the altitude at which maximum Z occurs, table 5 summarizes the comparison.

Table 5.- Correspondence Between Maximum Radar Reflectivities (Z) and Maximum Sferics (S)

Date	Number of Sectors With Both Maximum Z and Maximum α*	Number of Sectors With Both Maximum Z and Maximum S	Number of Times Max. Z and Max. S Were Adjacent or Together	Number of Sectors of Maximum Z
May 23	0	2	6	7
24	2	4	11	15
25	0	1	8	15
26	4	10	16	16
Total	6	17	41	53
	11%	32%	77%	100%

*α is the specific activity based on area: α = sferics level/echo area

The above comparison is biased from the standpoint that the locations of SPARSA and the radar were different so that the cloud volumes measured are not identical. The storm complex on May 26 was small, which may account for the greater degree of correspondence. In any event, maximum Z and S are quite closely related as evidenced by the fact that over 3/4 of the data located them within a two-sector angle, or 11°.

As will be discussed in the next section, large α values are usually associated with rapidly growing portions of a storm during the initial phases and especially in early stages of maturity of a storm before the sferics activity begins to decrease. The maximum α location agreement with maximum Z is the poorest.

2. *Quantitative Relationships*

Time and direction have been used in parametric form to relate both the radar and the sferics data to each other and to weather data. Because the sferics origin has been so well defined in terms of radar, it is possible to examine various quantitative relationships which may exist between them with respect to storm development and severe weather occurrences.

a. *Specific Activity*

In testing for correlation between the sferics level in a sector and the radar echo intersected, both the echo area, A, and effective length, L, have been quantized (see fig. 10). The absolute reflectance is not considered because, during the storm periods studied, distance change was negligible.

(1) *Specific activity based on area.* When the sferics level is divided by the intercept echo area, this ratio is defined as α in units of counts per minute per square mile, as previously stated. This is a normalization for the variation in storm volume included in a SPARSA sector with varying range. Large values of specific activity greater than 1.5 occur in different sectors and at different times. They are usually related to regions which show radar echo prior to the sudden increase in sferics which increases the sferics to echo area ratio, α.

Different storms show different distributions of α. In some, α rarely exceeds 1.5. This analysis has not been completed.

(2) *Specific activity based on length.* When the sferics level is divided by the mean length of the intercept echo area (see fig. 10), this ratio is defined as β in units of counts per minute per mile. This is a normalization for geographic orientation as well as a parameter of area. The sectors which intersect the cloud boundaries may have appreciable length but not much area. If this is an active or growing boundary, sferics activity will be distributed along the length and give rise to a high sferics count rate. This would result in a large value of α which is a consequence of quantizing of azimuth into sectors. In the same situation, β would present a more realistic measure of specific activity. Seventy miles appears to be the maximum cloud length intercepted, from all the data analyzed.

The SPARSA count rate is a function of both sferics activity in the sector detection volume and the sferics pulse amplitude distribution. When the sferics source is uniformly extended along the radius of a sector, the pulse amplitude distribution effectively shifts toward a larger proportion of smaller pulses due to propagation loss with increasing range. The significance of β is a function of range and intercept length. The analysis of β with respect to different storms has not been completed at this time.

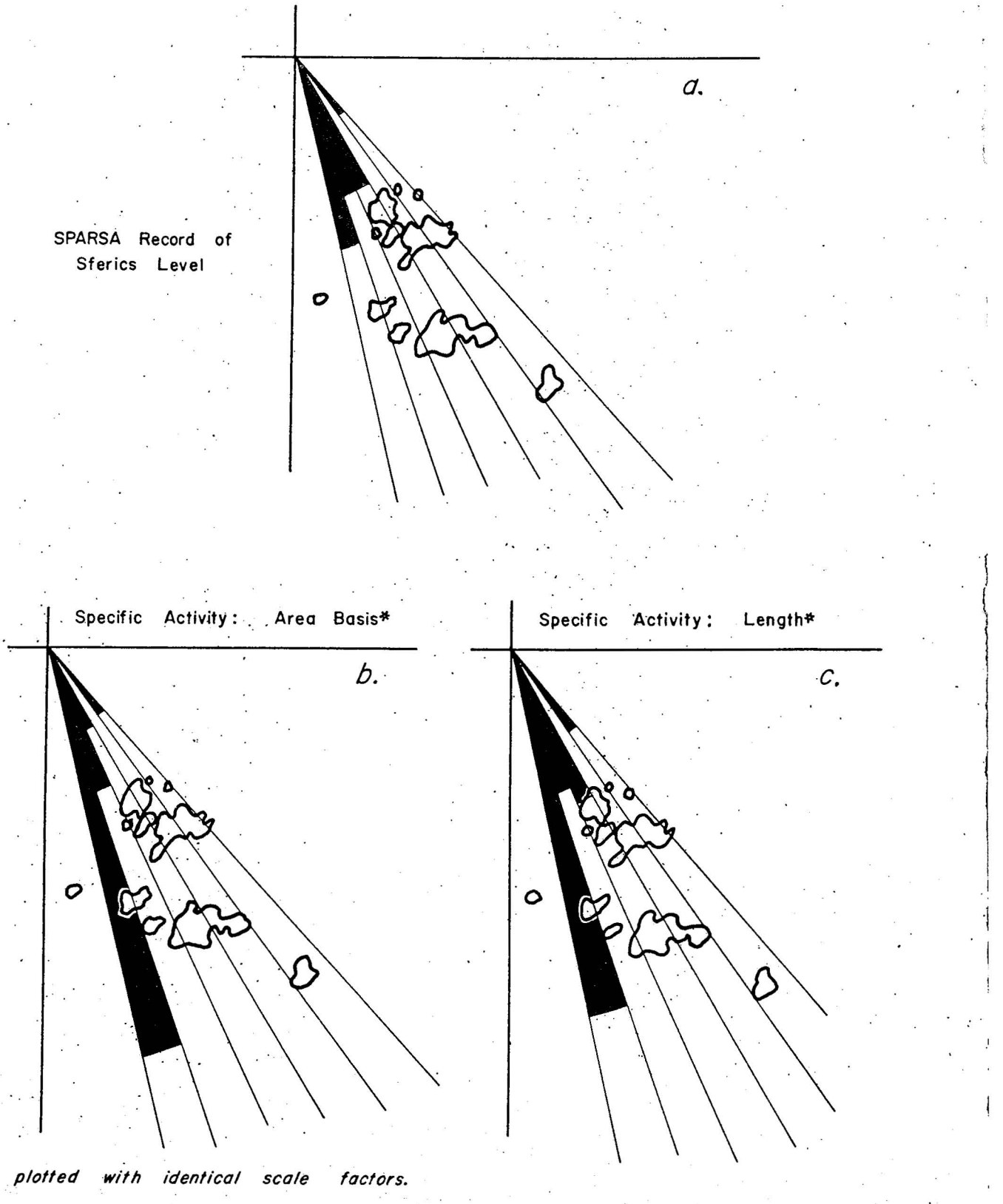

Figure 16.- Figure showing relative values of sferics count rates based on (a) total count, (b) specific activity (area bases) and (c) specific activity (length bases) for Shawnee at 1445 CST, June 11, 1962.

(3) *Interpretation of specific activity.* An example of the distinction between total sferics level, α and β, in terms of the actual radar echo is shown in figure 16. The polar plot of sferics level shown in figure 16a was taken from the series, of which figures 12 and 14 are a part, at 1445 CST, June 11. This indicates highest activity along the west edge of the storm complex, but in evaluating the relative activity of that sector, it is obvious that the next two adjacent sectors pass more directly through the storm and contain more echo area.

If lightning and electrification were proportional to area, then the significance of the activity in the west edge sector would be even greater because the area is considerably less. The proportionality of sferics level and area is the basis for defining α, and the resultant polar plot of α is given in figure 16b.

The plot of β in figure 16c also gives a large value to the west edge sector. When both α and β are in agreement, the specific activity distributions attain the most significance, but in an absolute sense the proportionality between sferics level and area or length must also be verified.

To further illustrate the relationships of these parameters during the development of a storm complex, an extended storm history is presented in figure 17.

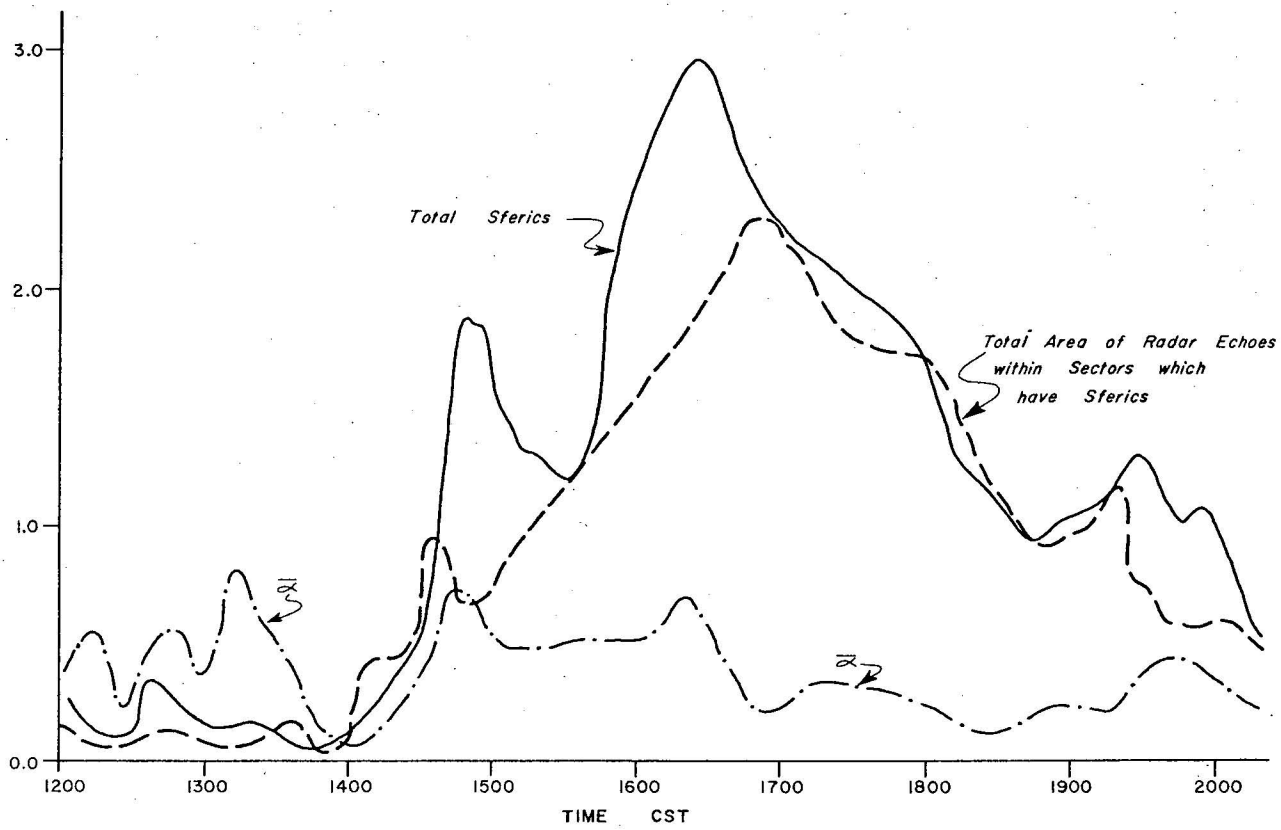

Figure 17.- Storm history for June 12, 1962, including total sferics, area, and specific activity α.

In figure 17 the variation in total sferics activity is shown for the period 1200 CST to 2020 CST. Also shown is the total cloud echo area within *only* those sectors which have sferics activity. It is important to note that the relationship between the total cloud area and the cloud area with sferics activity is continually changing. In this instance, the total radar echo area (not shown on graph) increased rapidly between 1330 and 1400 CST and continued to increase until 1830 CST. (This may also be stated on a sector basis as in fig. 11.) The area representing the sferics sources, however, shows a gradual increase and subsequent decrease.

The average specific activity, $\bar{\alpha}$, is shown for the entire period in figure 17. An increase in $\bar{\alpha}$ occurs when the total sferics level is increasing more rapidly than the total echo area. Six maximum points of $\bar{\alpha}$ occur at the same time as groups of sectors show simultaneous sferics maxima, as in figure 15. Their times are: 1205, 1250, 1320, 1450, 1615, and 1930 CST. There is a tendency for $\bar{\alpha}$ to remain constant during periods of sferics increase, even though some individual sector α values do achieve their greatest level then. This is due to the azimuthal distribution of activity which shows wide ranges of values, but with low mean level.

(4) *Correlation coefficients.* In order to derive a functional relationship between S, the sferics level or count rate, A, the radar echo area, and L, the radar echo length, it is necessary to handle the data for each sector separately because storm activity in different sectors may be in different stages of development. There is a general trend toward an increase in sferics related area, even after the maximum total count rate time has been passed. The data thus have been classified into two groups: sferics level increasing (positive slope) and sferics level decreasing (negative slope). A further distinction was observed by grouping the data according to sferics level less than or greater than 20 count rate units. In this way the initial activity processes, when sferics are first being generated, may be separated from later stages of development.

With a sample size of 281 measurements for June 12, the correlation coefficients were derived and are shown in table 6.

Table 6.- Correlation Coefficients: S, A, L for June 12, 1962

	Sferics Level Less Than 20 Units	Sferics Level Greater Than 20 Units	Composite	Sferics Activity Slope
r_{SA}*	+0.28	+0.67	+0.66	+
r_{SL}*	+0.29	+0.53	+0.51	+
r_{SA}	-0.11	-0.01	-0.03	-
r_{SL}	-0.10	+0.06	+0.02	-

*r_{SA} = correlation coefficient relating sferics count rate and radar echo area

*r_{SL} = correlation coefficient relating sferics count rate and radar echo length

The data included in table 6 are for an entire storm history from its initial sferics activity appearance. Correlation coefficients were computed for the storms on June 10 and June 11, also. Data for both storms begin late, however, after a considerable buildup period had taken place. The June 10 data begin with a total area of 910 square miles, which is decreasing steadily to 464 by the last measurement. The correlation coefficients obtained from 165 measurements showed a reversal in sign: $r_{SA} = -0.22$ for increasing activity and $r_{SA} = +0.25$ for decreasing activity, indicating possible variations in storm behavior. It is interesting that even during the later stages of activity decrease the low sferics levels are apparently associated with the formation of new cloud areas. For sferics level less than 20 units, the correlation coefficient for increasing sferics activity was: $r_{SA} = +0.75$, whereas the decreasing activity values gave: $r_{SA} = +0.02$. The lower level thus appears more reliable.

For June 12, 1962, the low level correlation coefficients, r_{SA}, for all three days were positive, as follows: +0.75, +0.23, and +0.28. The decreasing sferics activity grouping of the high level area and length correlation coefficients were all near zero, as follows: +0.06, -0.01, +0.03, -0.03, -0.06, and +0.03.

During the initial phase of general sferic activity increase, there appears to be a linear relationship between the increase in sferics and the increase in radar echo. Careful examination of the data shows, however, that there are often short-term increases in sferics level which are significant, but because they represent a small part of the overall buildup, their effect on the correlation is minimal. The change in α which this increase represents is of importance in relating the sferics level to absolute reflectance, as mentioned in the following section.

b. *Absolute Reflectance*

The radar-reflectivity factor Z* was determined in the conventional manner by measuring the amount of receiver attenuation (step gain) necessary to extinguish the persistent echo, the range, and the altitude. All of the SPARSA sectors intersecting the subject cloud were identified as well as the sector corresponding to the final hard echo location (maximum Z). Analysis of the specified sectors on the recordings gave the appropriate sferics count rate data.

The graphs, as seen in figures 18 and 19, show:

(a) The time history of the sferics count rate (S_Z) in the maximum Z sector. It is important to note that the two periods studied here were both at the beginning of long and intensive periods of sferics and severe storm activity.

(b) The time history of the maximum sferics count rate (S_M) in the specified cloud SPARSA sectors. The S_Z graph shows how S varies in the same location as Z_M, while this graph shows how S_M varies for the study cloud.

*The radar-reflectivity data were obtained from Mr. Neil Ward, research meteorologist, U. S. Weather Bureau (NSSP), who performed the necessary analysis on the radar films to compute the Z factors.

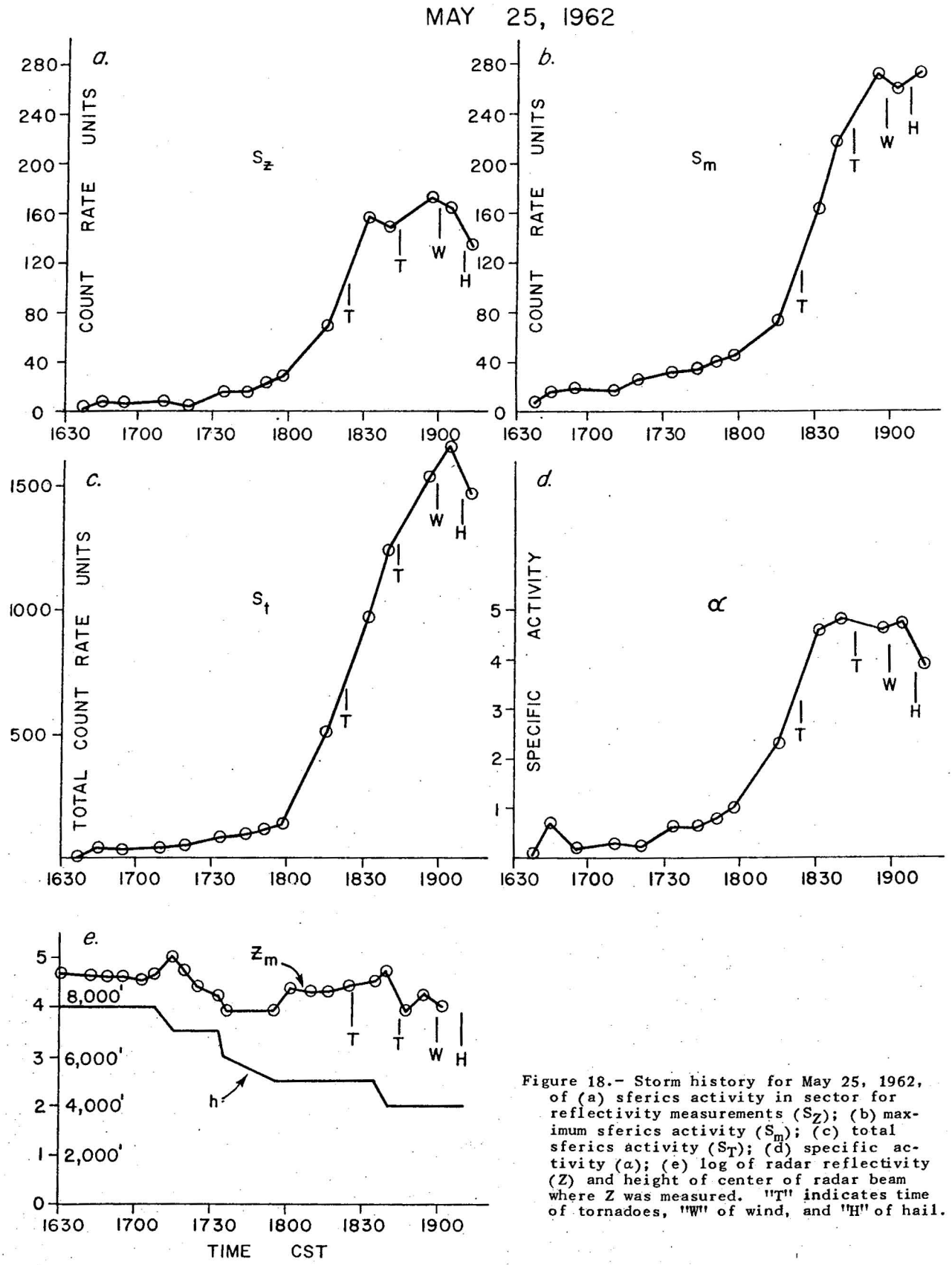

Figure 18.- Storm history for May 25, 1962, of (a) sferics activity in sector for reflectivity measurements (S_Z); (b) maximum sferics activity (S_m); (c) total sferics activity (S_T); (d) specific activity (α); (e) log of radar reflectivity (Z) and height of center of radar beam where Z was measured. "T" indicates time of tornadoes, "W" of wind, and "H" of hail.

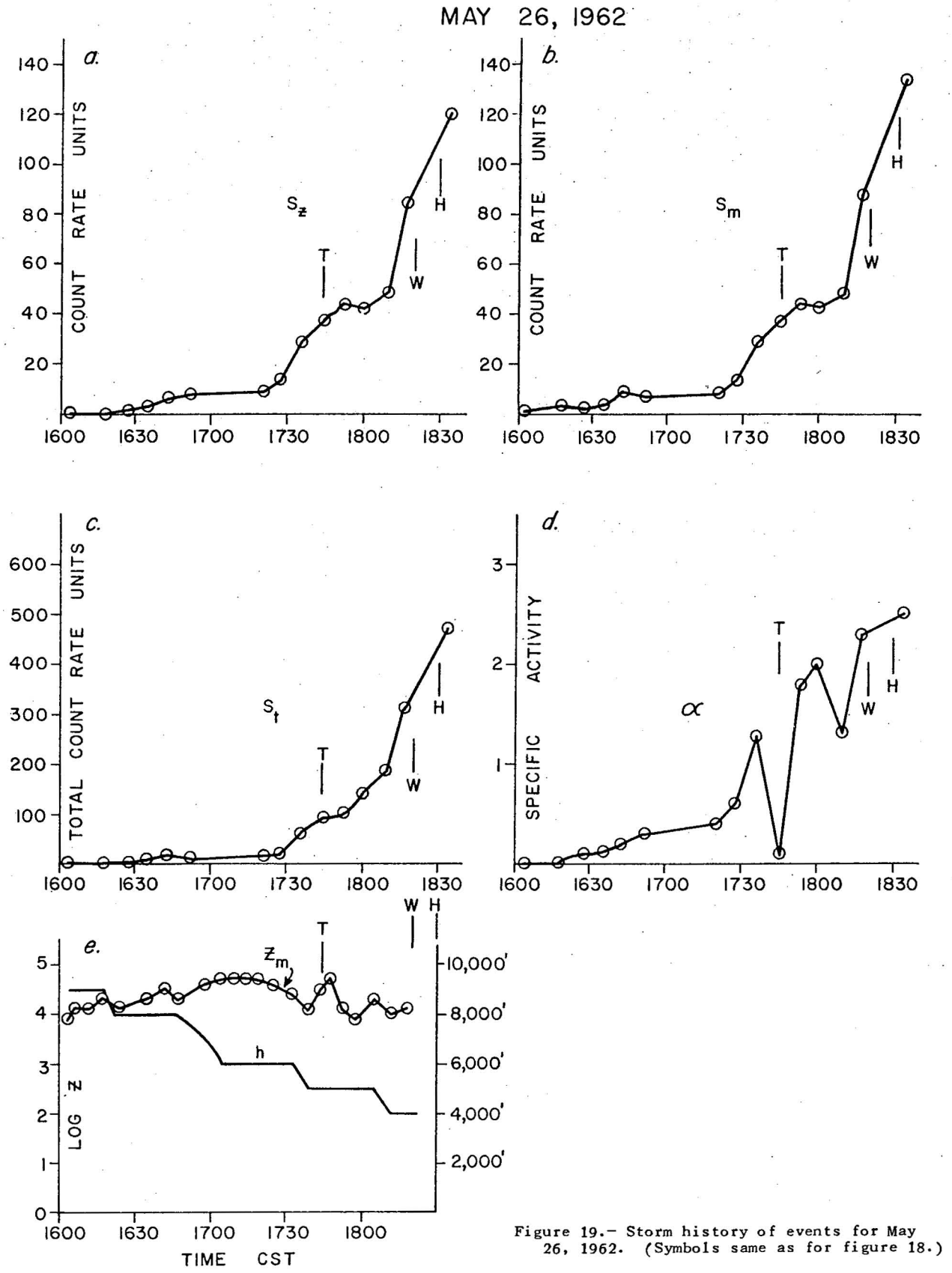

Figure 19.– Storm history of events for May 26, 1962. (Symbols same as for figure 18.)

(c) The time history of the total sferics count rate (S_T) for all the specified cloud sectors. This graph shows the entire cloud activity variation during the analysis period.

(d) The time history of the specific activity (α - counts/min./sq. mi.) for the specified maximum Z sector.

(e) The time history of the log Z (Z is the radar-reflectivity factor) and the time history of the height of the center of the radar beam at the range of Z_M point. No vertical radar scans were made; thus, the Z value may have been greater at higher elevations, but no sector shift is expected.

It is obvious from a study of the above graphs that there is very little similarity between the histories of the radar reflectivity, sferics count rate, and specific activity. However, it is important to note that the rate of increase of S, S_M, S_T, and α is large and rapid during the time of the severe weather events. The changes in log Z are not large, nor do they seem to coincide with the times of the severe weather activity.

The relationship between the location of log Z_M and S_M were noted. The storm histories of log Z_M and sferics parameters are greatly different. The location of the Z_M point and the S_M point in a cloud, however, are adjacent, and they are seen to move from one part of the cloud to another at nearly the same time.

c. *Severe Weather Activity*

In Section III, C, 2b, it was shown that the severe weather events occurred during the buildup of the sferics activity (figures 6, 9, 18 and 19). It was also noted that the periods under study were at the beginning of long and intensive sferics and severe weather periods.

The discussion of Section III, C, 1c (fig. 15) showed that the omni-directional total sferics count rate was composed of the summation of the count rate in all SPARSA sectors. It was noted that the points of maximum in the individual sector time histories occurred at the same time as the maxima points occurred on the total sferics count rate recording. The omni-directional total sferics count rate history is, therefore, seen to be a true summation of all the storms in the detection range. A study of total sferics count rates for May 23, 24, 25, and 26 was made and the data compared with the severe weather events.

A summary is shown in table 7. A study of this table shows that a very large percentage (84%) of the severe weather events occurred during the initial overall increasing total sferics activity while only 16 percent occurred when sferics activity was decreasing.

3. *SPARSA Triangulation*

The common area of detection for both SPARSA units was about 70,000 square miles or 60 percent of a single station coverage. Storms located within this area and observed by both stations were used to test triangulation on

the basis that the intersection area defined by an azimuth sector from Shawnee and one from Arapaho must include radar cloud echo. The data in table 8 summarize the limited amount of analysis performed to date.

Table 7.- Severe Weather Incidence Related to Total Sferics Activity

Date and Time of Investigation	SW Events Occurring Prior to S_T Maximum	SW Events Occurring After S_T Maximum	Total Number of SW Events
1500 CST May 23, 1962 to 0600 CST May 24, 1962	4	0	4
1600 CST May 24, 1962 to 0440 CST May 25, 1962	25	5	30
1620 CST May 25, 1962 to 0800 CST May 26, 1962	14	5	19
1500 CST May 26, 1962 to 0810 CST May 27, 1962	13	1	14
Total	56	11	67
	84%	16%	100%

Table 8.- SPARSA Triangulation Summary

Date	Number of Sectors With Sferics and Common Intersections With Radar Echoes	Number of Sectors With Sferics but No Common Intersections With Radar Echoes	Total Number of Sectors With Sferics
June 18	18	6	24
18	30	0	30
25	15	19	34
27	23	8	31
27	24	10	34
27	17	10	27
Totals	127	53	180
	70%	30%	100%

The use of averaged count rate data does have triangulation limitations which are not common to real-time systems. Time did not permit a thorough analysis of even these few examples because it is necessary to calculate the effective common volumes (area) in such a way as to compensate for different solid angles which the same storm subtends to each SPARSA location. Although the count rate is independent of distance, different portions of the storm are monitored so that the triangulation can never be perfect.

The biggest problem discovered in the attempt at triangulation is due to the SPARSA's 180° ambiguity which makes triangulation difficult for all but simple situations. It should be noted, however, that when the weather radar echo locations are known in advance, triangulation, even without directional sense circuitry, is not too difficult. Refer to figure 20 for an example of indications from both SPARSA sets at the time of a funnel-cloud report.

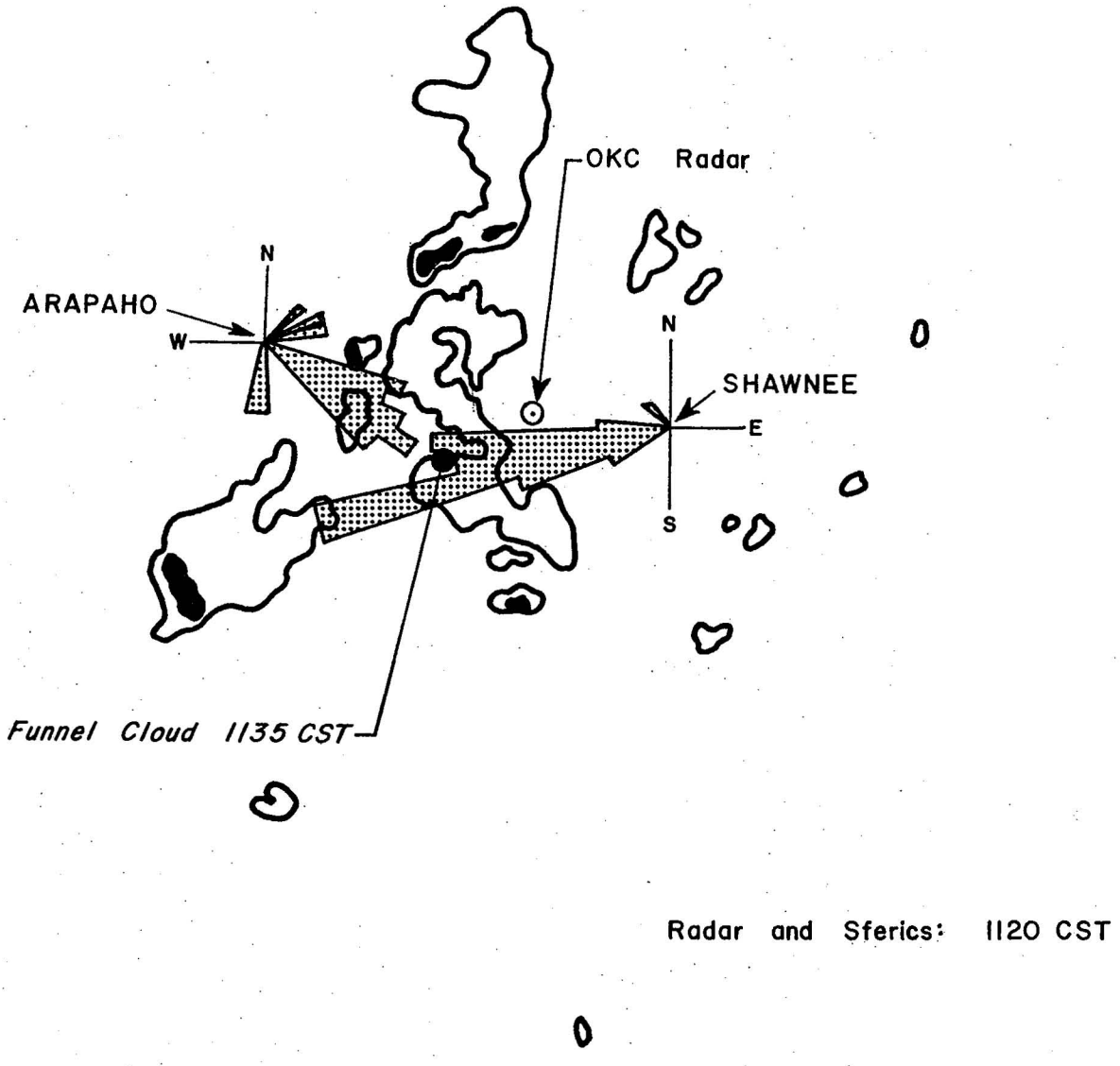

Figure 20.- Example of SPARSA triangulation. Cross-hatched area indicates relative sferics activity. Solid block areas indicate area of very strong radar return.

IV. MISCELLANEOUS OBSERVATIONS

Limitations in the scope of the instrumentation used in the field as well as the level of effort have not permitted proper documentation of certain important observations involving 500-kc. sferics. Some of these will be mentioned, however, in order to make this report more complete.

A. INITIAL ELECTRIFICATION STAGES OBSERVED BY 500-KC. SFERICS

There were a number of instances when a cumulus cloud undergoing rapid vertical development was situated overhead within three miles of the SPARSA location. Personnel at the sites were able to relate a series of short-duration 500-kc. sferics pulses to the single cloud development.

The time interval between pulses would initially be nearly 4 seconds and would gradually decrease in avalanche fashion much like the onset of "popping" in a roaster full of popcorn. In some instances the avalanche of pulses would be terminated by a single visible lightning flash and thunder after which the cloud development ceased. The vertical development stopped, and the cloud became ragged in appearance.

None of the "popping" sferics was accompanied by any evidence of lightning or thunder. On some occasions the vertical development continued along with a repetition of the avalanche phenomenon. In every instance, the lightning would terminate one series of 500-kc. pulses and begin a new series. The time interval between the main electrical discharges, or lightning, also began to decrease with increasing vertical development. It is estimated that the earliest onset of "popping" signals occurred before the cloud tops reached the freezing altitude.

B. QUASI-CUMULONIMBUS CLOUD FORMATIONS

Frequently, there were days during which towering cumulus formations would fill the entire sky. Cloud tops would exceed 20,000 feet (estimated), and even some precipitation was in evidence. The only visual distinction between these clouds and an active cumulonimbus formation is the evidence of a slightly ragged appearance on the tops of the ascending turrets. The 500-kc. sferics indication during these false cumulonimbus developments was zero.

C. STORM SIZE AND 500-KC SFERICS DYNAMICS

The general characteristic of sferics activity associated with thunderstorm periods is a rather symmetrical buildup-decrease function with a well-defined maximum point. It has been demonstrated that the radar echo originating sferics continues to increase after the total sferics activity passes the maximum point. The interval which exists from the time of total sferics maximum to the time of maximum sferics-emanating cloud echo area appears to be proportional to the overall extent of the storm area.

V. SUMMARY AND CONCLUSIONS

Previous investigations [5, 6] showed that monitoring sferics on 500-kc. results in a detection system which has a well defined maximum range and zero fair weather response. The use of this frequency in the study of severe weather associated with thunderstorms has shown evidence of the intimate relationship between the electrification processes and dynamics of severe storms.

Certain questions were posed in the introduction which were used as a guide in the data analysis in order that the answers might be derived. The answers indicated by the data analyzed so far are as follows:

1. Severe weather, as defined by U. S. Weather Bureau reports of wind, hail, and tornado damage, does not occur without 500-kc. sferics activity. None of 191 reported severe weather events occurred without sferics activity somewhere in the detection range.

2. The number of severe weather (SW) events is proportional to the total sferics activity. (Correlation coefficient = +0.51). In only 2 percent of the SW events did sferics fail to be detected coming from their exact location, and these were at the limit of range. The ranges over which SW events were detected by sferics extended from 5 to 240 statute miles.

   Most severe weather (84%) occurs during the rapid sferics buildup period prior to the storm period maximum, even though radar evaluation may indicate storm maturity to the level of the formation of hard echoes a considerable time prior to the sferic buildup. Also, a decreasing sferics trend precedes the storm dissipation trend.

3. Ninety-eight percent of the 500-kc. sferics activity originates in cloud regions definable as radar cloud echo. Four percent of the time sferics activity precedes the buildup of a cloud echo into area previously devoid of echoes. Less than half of the radar echoes produce sferics activity.

4. The most intense precipitation indicated by maximum Z, or radar reflectance, is located in the vicinity of maximum sferics activity during the buildup stages of a thunderstorm. Other areas of high sferics activity are rapid buildup portions of a storm unrelated to the location of maximum Z. Maximum buildup regions may be given quantitative ratings in terms of specific activity during the incipient stages.

5. An increasing sferics count rate is related to the general maturity increase in a thunderstorm as evidenced by the onset of the severe weather manifestations or precipitation formation during this period. The sferics activity changes result from large area fluctuations rather than individual thunderstorm cell developments. The fluctuations are such that a 2-hour history is necessary to make a 98 percent accurate prediction of overall regional storm trends.

The time needed to make an accurate prediction of the trend for a small portion of a single storm is considerably less than 2 hours and decreases with increasing slope of the sferics activity.

The changes of maximum radar reflectance and sferics activity during the increasing stage of the storm are apparently not related. Radar evidence of cloud formation, as well as the detection of hard echo regions, can *precede* the general increase in sferics activity.

From the preceding summary it appears that 500- kc. sferics may be produced by the electrification which exists in the region of "hard building" in a thunderstorm as well as in the region of intense precipitation. Fitzgerald [7] has reported high fields and uniform negative charge next to vertical cloud walls. The SPARSA indications are high from these regions. As pointed out previously, these active regions are not related to the maximum radar reflectance, but there is high sferics activity associated with the bright echo region where the electrification is even greater.

The vertical turbulence associated with the boundary of the bright echo, and the rapid buildup portions of the storm may thus, perhaps, because of or due to the high electrical charge, give rise to much 500-kc. sferics activity.

The relationship between the lateral extent of a storm and its 500-kc. sferics level does not have particular meaning because the ratio of sferics to area is constantly changing. Further, the existence of regional changes in sferics activity adds uncertainty to forming such a relationship.

Finally, the thunderstorm is a transformation of latent thermal energy which, due to the localized area of influence, apparently becomes stable in its self-generation-regeneration process after a short period of development. Sferics count rate appears to be a good indicator of "power level" of the process.

REFERENCES

1. U. S. Air Weather Service (MATS), "Project Tornado-Sferics." Final report, ASTIA AD 218-741, 1957.

2. U. S. Air Weather Service (MATS), "Project Tornado-Sferics 1960 Phase." Final report, ASTIA AD 254-827, 1961, p. 16.

3. Jones, H. L. and Kelly, R. D., "Research on Tornado Identification: Compendium for Period 1 January 1952 to 31 December 1956," Signal Corps Contract DA-36-39-SC-64436, Oklahoma A and M College, 1957.

4. Malan, D. J., "Radiation from Lightning Discharges and Its Relation to the Discharge Process," *Proceedings of the Second Conference on Atmospheric Electricity, Portsmouth, New Hampshire, May 20-23, 1958*, Pergamon Press, 1958, pp. 557-563.

5. Kohl, D. A., "Short Term Weather Forecasting Using Atmospheric Electrical Phenomena," *Scientific American*, vol. 200, No. 3, March 1959, p. 155.

6. Kohl, D. A., "Sferics Amplitude Distribution Jump Identification of a Tornado Event," *Monthly Weather Review*, vol. 90, No. 11, November 1962, pp. 451-456.

7. Fitzgerald, D. R. and Byers, H. R., "Aircraft Electrostatic Measurement Instrumentation and Observations of Cloud Electrification." Final report, AFCRL-TR-62-805, February 28, 1962.

USCOMM-WB-DC